CHAPTER V

Spectral Response, Rise & Decay of Photocurrent and Optical Properties

Chapter V

Spectral Response Rise & Decay of Photocurrent and Optical Properties

5.1 Introduction

Optoelectronic properties of semiconducting materials depend considerably on the wavelength as well as intensity of the incident illumination. From the related studies information regarding the recombination processes and carrier excitation mechanism may be obtained. Spectral response, rise and decay characteristics, transmittance and absorbance are some important physical attributes, which needs to be characterized properly.

Generally photoconductive materials show spectral distributions which exhibit sharp peaks in the vicinity of absorption edges when one proceeds from low energy to the high energy side of the absorption edge. In the same energy region along with this sharp peak some smaller peaks are also observed. In evaporate thin film photoconductors, the peak of the spectral response curve is generally found to be broadened.

The optical absorptions in thin films depend; apart from the wavelength and intensity of illumination, on structural parameters viz grain boundary potential, grain size, their orientations. Several workers reported the shifting of the absorption edge to the longer wavelength region for doped films /1,2/. The observed peaks in the long wavelength region of the absorption spectra are also attributed to the intensity of band transitions. Moreover the shifting of the absorption edge to shorter wavelength side may depend either on the indirect transition probabilities or degeneracy in a highly doped semiconductor films /3,4/.

When a photoconductor is exposed to light radiation, the photo current takes some time, the rise time, to reach the maximum or the steady state and when the illuminating radiation is turned off, photocurrent decays to reach the initial dark value within an another interval of time, the decay time. The particular growth and decay processes in a photoconductor can be explained in terms of the process of release of new electrons and holes, under illumination followed by their recombination /5,6/. When a photoconductor is exposed to radiation of suitable photon energies, electron-hole pairs are generated and their densities tend to increase with the time. The increase of carrier density due to photo

generation is controlled by the recombination processes and thus, a steady state is established when the rate of recombination becomes equal to the generation rate. After the light is turned off, photocurrent decays due to recombination of excess carriers.

The presence of traps plays a significant role in the control of growth and decay of photocurrent in polycrystalline thin film photoconductors. Polycrystalline thin film comprises of grain of various sizes along different orientations /7/, the grain boundaries separating the grains are disordered regions and contains trapping centers. These traps can capture electrons and holes; also detain them in restricted volume and time. When the sample is exposed to radiations a certain proportion of optically generated free carriers are captured by these traps. The filled traps will be emptied after switching off the light at a rate depending upon their cross section and the ionization energy. Thus the decay time will be different depending upon the trap depth, trap distribution etc.

This chapter embodies the results of experimental studies on rise and decay characteristics of CdSe thin film photoconductors for different intensities of illumination and wavelength for films with different thin film characteristics.

5.2 Experimental

The CdSe films were illuminated with the help of a 250 watt tungsten halogen lamp, which was operated at 24 volt, using a parabolic reflector. A series of Carl Zeiss (GDR) metal interference filters were used to obtain the required monochromatic illuminations. The intensity of illuminations was measured with the help of an Aplab sensitive lux meter (5011 S). A constant photon flux density was maintained during different experimental observations, for each selected wavelength by keeping the intensity fixed at a particular value. The dark current and the photocurrent were measured using an ECIL electrometer amplifier (EA 815) as described in chapter II.

The experimental CdSe films were of very high dark resistivity. So care needed to be taken to suppress the electrical noise generated by other sources. To eliminate the effect of stray radiations, observations were recorded at complete darkness, preferably at night. The spectral responses of photocurrent were studied for different monochromatic illuminations within the range of visible wavelength keeping the intensity fixed at a

definite value. This was repeated for different bias voltages and also under different intensity levels of illuminations.

The growth and decay characteristics of photocurrent were investigated under different levels of illuminations, bias voltages and at different ambient temperatures. The growth of photocurrent was observed by exposing the sample to light with the help of mechanical shutter and simultaneously recording the d.c. current for a definite time period. After some time of reaching the saturated state, the light was cut off and the decay of current with time was similarly recorded. An electrical heater connected with a stabilized power supply was used to raise the temperature of the thin film sample for taking observations of rise and decay of photocurrent at higher ambient temperatures. The corresponding temperatures were measured using a copper constantan thermocouple connected with a highly sensitive digital microvoltmeter.

For the study of optical properties of CdSe films in addition to the usual films few set of films with relatively higher thickness were prepared. The optical absorbance and transmittance of the films were recorded within the wavelength range 300-900 nm using a double beam varian uv-visible spectrophotometer. The glass plates, cut in proper sizes, used as substrate for deposition of the films, were used as reference.

5.3 Results and Discussions

5.3.1 Spectral Response

The spectral response characteristics (SRC) in a photosensitive semiconductor are a manifestation of optical absorption characteristics. Optical absorption in semiconductor may be classified broadly into four groups (i) 'fundamental' absorption associated with excitations across the energy gap. (ii) absorption due to the presence of conduction carriers, electrons or holes or both (iii) absorption associated with the electrons or holes transitions to or from the corresponding defect energy levels and (iv) absorption due to the excitation of the lattice vibrations, phonons /8/.

The first two types of absorptions are directly related to the electron energy band structure of the material, whereas the third type depends on the lattice imperfections such as impurities or the lattice defects. The excess photo generated carriers created in a semiconductor must eventually recombine either by radiative or non-radiative

recombination processes depending upon the transition probabilities. It is likely that the electron and the hole will recombine non radiatively through a defect center and the excess energy is dissipated into the lattice as heat /9/.

In direct transition, an electron rise from the top of the valanced band to the bottom of the conduction band due to the absorption of a photon without change in momentum. There is a small change in k (wave vector) due to finite momentum of the photon, which is equal to h / λ. An indirect transition involves a large change in the momentum and occurs by the emission or absorption of different type of phonon depending upon the mode of lattice vibrations /10,11/.

Several workers studied the photon associated transitions in CdSe thin films /12/. Such experiments provide information regarding the band gap, direct and indirect transitions and the energy position of defects and impurity levels.

5.3.2 Spectral response characteristics in CdSe thin films

The degree of crystallization, absorption edge and the impurity levels of the semiconductors can be estimated from the spectral response studies. The spectral response characteristics of thermally evaporated CdSe thin films having same thickness 2000Å, but grown at T_s = 423K, 473K, and 523K are presented in the Fig 5.1(a). The maximum photocurrent is observed in each case, at a wavelength of 725 nm and this is found to be independent of T_s. Similar results are also observed for the films having different thickness 1750Å, 2100Å and 2230Å but grown at the same T_s = 473K, as shown in the Fig. 5.1(b). For all these observations the intensity of illuminations were kept at a certain fixed value.

Resembling observations of spectral response characteristics of a CdSe film under different applied bias conditions and also under different intensity of illuminations are shown in Fig 5.1(c) and Fig 5.1(d) respectively. The maximum value of photocurrent in case of the prominent peak is found to increase with T_s and, t. Similar increase is also observed with applied bias and intensity of illuminations. The increase of photocurrent with increase of T_s and thickness of film is mainly due to improvement of crystallinity along with the increase of grain size. Higher grain sizes can decrease the grain boundary potential barriers in these films and enhances the carrier mobility /13/.

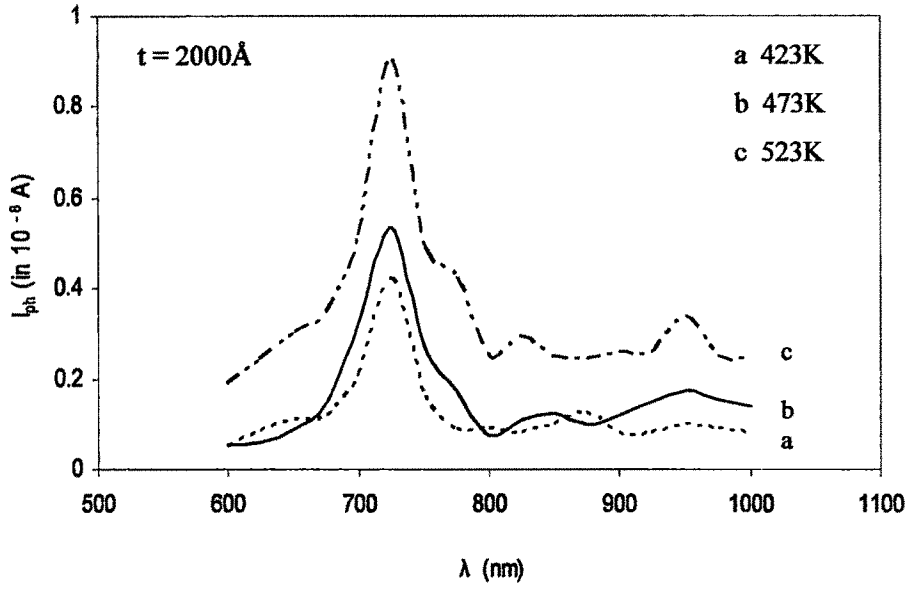

Figure 5.1(a) Spectral response characteristics of CdSe thin films of same thickness and grown at different elevated T_s.

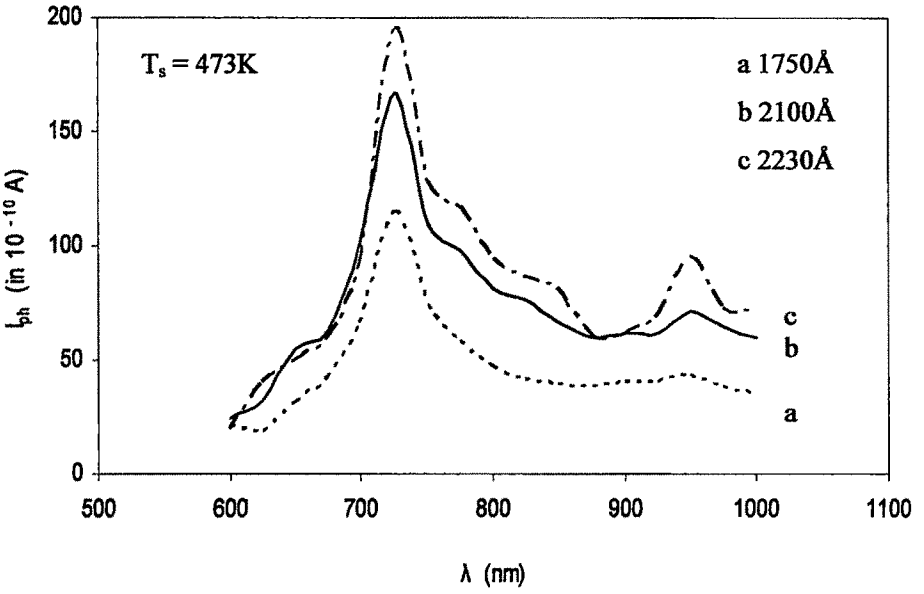

Figure 5.1(b) Spectral response characteristics of CdSe thin films of different thickness and grown at same elevated T_s.

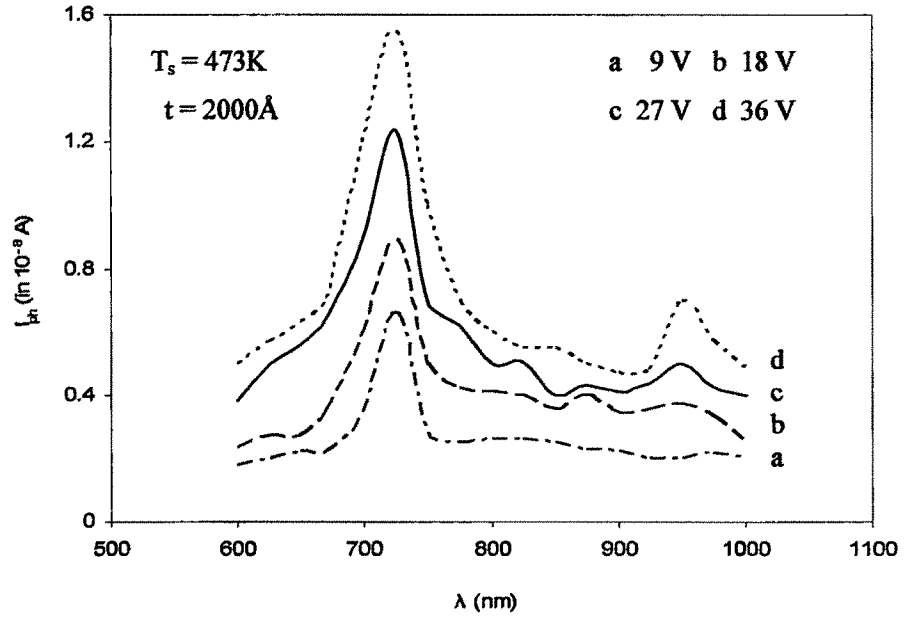

Figure 5.1(c) Spectral response characteristics at different applied bias of a CdSe thin film of constant thickness and grown at elevated T_s.

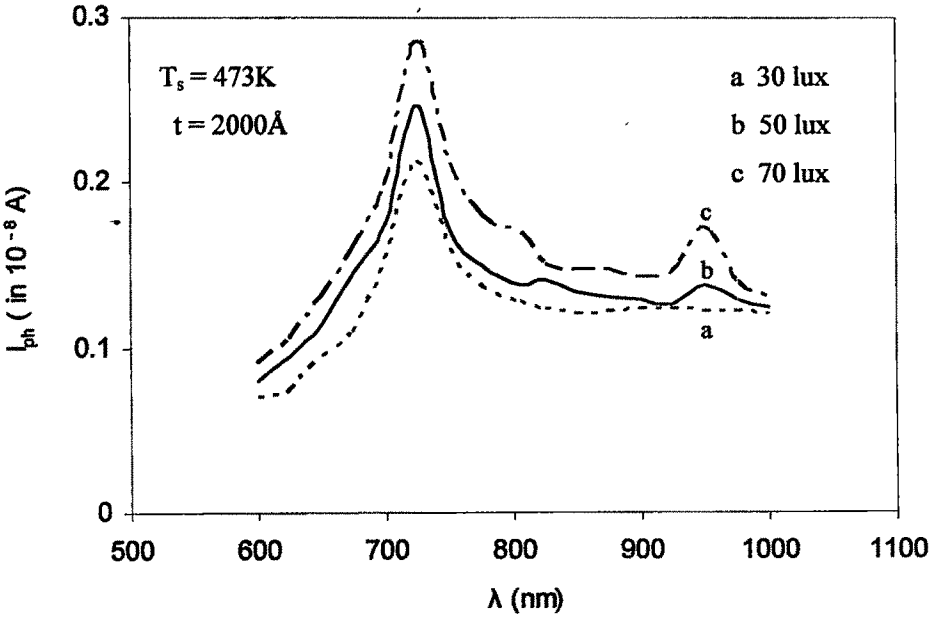

Figure 5.1(d) Spectral response characteristics under different intensity of illuminations of a CdSe thin film of constant thickness and grown at elevated T_s.

From the observations of the spectral response curves it can be inferred that in case of CdSe thin films the maximum absorption occurs at around λ = 725 nm. The photocurrent is less in the short wavelength side but an additional peak on the longer wavelength side at around 950 nm is observed. The observed optical band gaps corresponding to these wavelengths are found to be 1.71 eV and 1.3 eV respectively. The optical absorption edge for CdSe thin films at 1.71 eV is due to the direct transition of the electrons from the valanced band to conduction band /14-16/. The additional defect levels associated with the transition at 950 nm are estimated as 0.41 eV. This energy level may be attributed to the native defects in CdSe thin films /17,18/.

It is observed that there is a decrease in the photocurrent for both wavelengths, shorter and longer than the band edge wavelength. For longer wavelengths it may be explained on the basic of high optical transmittance and low absorbance of light. The shorter wavelengths have higher photon energy and are strongly absorbed and so produce excitation only near the thin surface layer of the film. The surface imperfections are characterized by rapid non radiative recombination, the excitation of photoconductivity being less when limited to the surface /19,20/. Since the volume of this layer is small, the concentration of free carriers (both electrons and holes) in it become very high which causes sharp increase in the recombination rate and hence decreases the surface life time. The increase in the recombination rate is also facilitated by the presence of various impurities and defects in the surface layer, which act as a recombination centers /21/. Thus due to high surface recombination photocurrents are smaller.

5.3.3 Photocurrent rise and decay characteristics

The phenomenon of rise and decay of photocurrent may be analyzed from the following consideration /22/. The recombination rate of excess carriers in CdSe thin films is given by

$$R_n = - \Delta n / \tau \qquad (5.1a)$$

$$R_p = - \Delta p / \tau \qquad (5.1b)$$

where Δn and Δp are the densities of excess carriers (electrons and holes) and τ is the photoconductivity growth time. The total change in the number of excess carriers in a given time interval is the sum of the rates of their formation and recombination /23,24/

$$d(\Delta n)/dt = G_n + R_n = \alpha\eta\Phi - \Delta n / \tau \tag{5.2a}$$

$$d(\Delta p)/dt = G_p + R_p = \alpha\eta\Phi - \Delta p / \tau \tag{5.2b}$$

where G_n and G_p are the rate of carrier formation, η is the quantum yield, which determines the average number of electron hole pairs generated by a quantum hv of radiant energy, α is the light absorption coefficient and Φ is the intensity of light . The solution of equations (5.2a) and (5.2b) may be written as,

$$\Delta n\, e^{t/\tau} = \tau\, \alpha\, \eta\, \Phi\ e^{t/\tau} + c \tag{5.3a}$$

$$\Delta p\, e^{t/\tau} = \tau\, \alpha\, \eta\, \Phi\ e^{t/\tau} + c \tag{5.3b}$$

where c is the integration constant. For growth of current $t = 0$, $\Delta n = 0$

Hence $$c = -\tau\, \alpha\, \eta\, \Phi$$

So equation (5.3a) becomes

$$\Delta n = \tau\, \alpha\, \eta\, \Phi\ \{1 - e^{-t/\tau}\} \tag{5.4a}$$

Similarly $$\Delta p = \tau\, \alpha\, \eta\, \Phi\ \{1 - e^{-t/\tau}\} \tag{5.4b}$$

The time dependence of the growth of the photoconductivity, σ_t , is given by

$$\begin{aligned} \sigma_t &= e\, \mu\tau\, \alpha\, \eta\, \Phi\ \{1 - e^{-t/\tau}\} \\ &= \sigma_o\{1 - e^{-t/\tau}\} \end{aligned} \tag{5.5}$$

For $t = 0$, $\sigma_t = 0$, and for $t \to \infty$, $\sigma_t = e\, \tau\, \mu\, \alpha\, \eta\, \Phi = \sigma_o$

where μ is the carrier mobility and e is the charge.

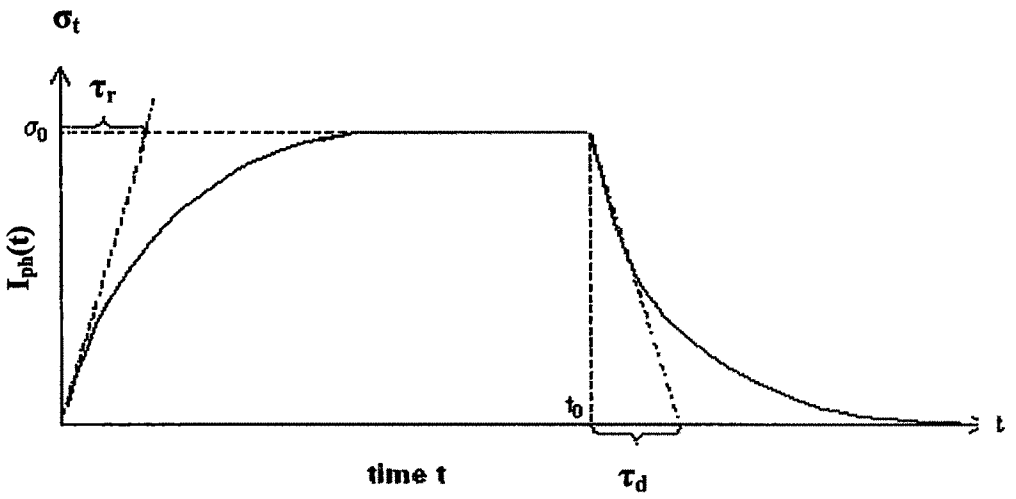

Figure 5.2 Rise and decay of photocurrent, $I_{ph}(t)$, of photoconductor after turning on and off the light source.

The plot of the photoconductivity function versus time, t, given by equation (5.5), for the growth of current, yields a curve as shown in the first part of the Fig 5.2. The tangent to this curve at the origin of the coordinate system intercepts the straight line $\sigma_t = \sigma_0$, at $t = \tau_r$ which corresponds to the photoconductivity growth time.

After a lapse of time, when the photocurrent reached a steady state value, the illumination is turned off and then the photocurrent begins to decrease. The change in the number of excess carriers occurs as a consequence of their recombination. Hence

$$d(\Delta n)/dt = -\Delta n / \tau \tag{5.6a}$$

$$d(\Delta p)/dt = -\Delta p / \tau \tag{5.6b}$$

Taking the origin of the scale at, t_0 (Fig 5.2), at the instant of turning off the illumination, the concentration of the excess carrier is given by

$$\Delta n = \alpha \eta \Phi \tau \tag{5.7}$$

With this condition (5.7), equation (5.6a) has the solution to be given by

$$\Delta n = \tau \alpha \eta \Phi e^{-t/\tau} \tag{5.8}$$

The time dependence of decay of photoconductivity is given by

$$\begin{aligned} \sigma_t &= e \mu \tau \alpha \eta \Phi e^{-t/\tau} \\ &= \sigma_0 e^{-t/\tau} \end{aligned} \tag{5.9}$$

The next part of the curve, shown in Fig 5.2, is obtained by plotting the function given by equation (5.9) against time. The decay time is obtained by drawing the tangent to the curve at the point t_0 and intercepts the time axis at t gives the decay time $\tau_d = t - t_0$.

Figs 5.3 (a to d) and Figs 5.4 (a to d) show the curves of experimentally observed rise & decay of photocurrent, $I_{ph}(t)$, as a function of time, for films of constant thickness and T_s, at room temperature and at higher ambient temperatures respectively. The curves of Figs 5.3(a to c) represent the growth and decay characteristics for different wavelengths as well as intensity of illuminations, under constant applied bias, at room temperature. Single set of observation was taken for different applied bias conditions keeping the intensity of illumination and wavelength constant [Fig 5.3(d)]. Observations were also taken keeping the sample at different ambient temperatures to see the contribution of carrier in the photocurrent decay due to thermal trap emptying process. These plots are shown in Fig 5.4(c) and Fig 5.4(d). The natures of the curves are similar to that shown in Fig 5.2, obtained from theoretical plot. Fig 5.4(a) and Fig 5.4(b) show alike plots under low and high intensity of white light illuminations at room temperature respectively.

Photocurrent rise and decay characteristics in the films may be explained on the basis of generation of excess carriers due to photon absorption for $h\nu > E_g$, (as well as thermal excitations) followed by their recombination. Since both bimolecular and monomolecular recombination predominant in the present experimental films so it is in accordance with the picture of trap being present in the energy gap in the band model leading to the charge carrier generation by the optical and thermal excitation processes.

From the Fig 5.3(c) and Figs 5.4(a to d) it is observed that values of τ_r and τ_d are dependent on intensity of illuminations. These values decrease with increasing intensity.

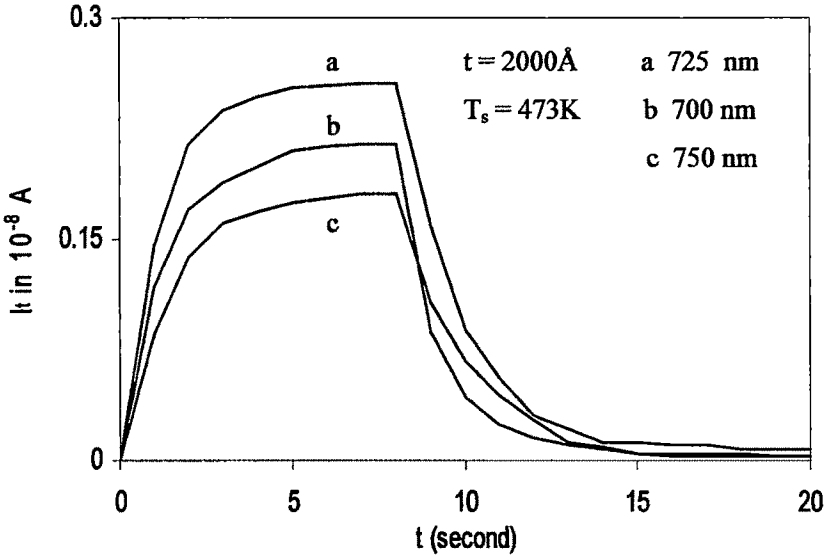

Figure 5.3(a) Growth and decay of photocurrent, $I_{ph}(t)$, of a CdSe thin film grown at elevated T_s and illuminated by monochromatic lights.

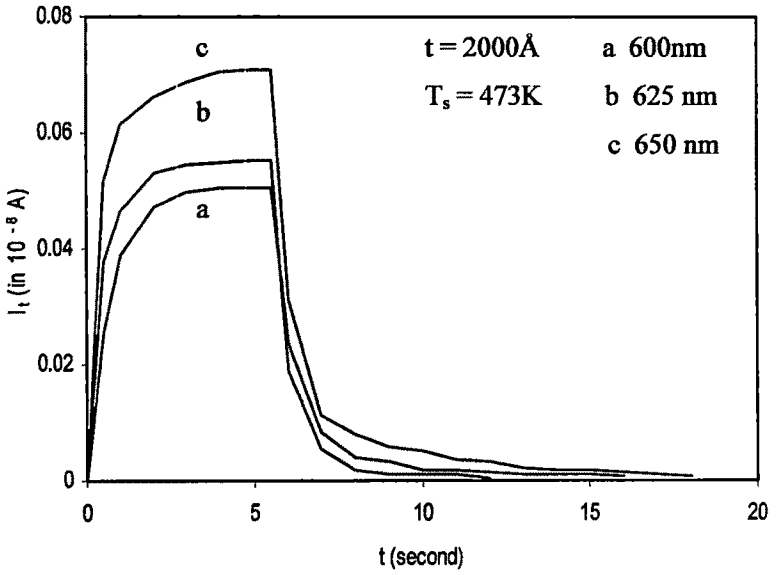

Figure 5.3(b) Growth and decay of photocurrent, $I_{ph}(t)$, of a CdSe thin film grown at elevated T_s and illuminated by monochromatic lights.

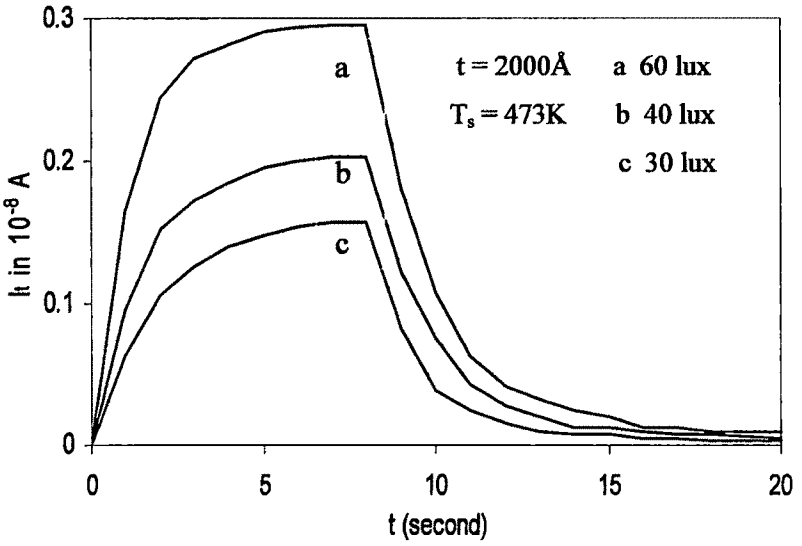

Figure 5.3(c) Growth and decay of photocurrent, $I_{ph}(t)$, of a CdSe thin film grown at elevated T_s and illuminated by monochromatic light (725nm).

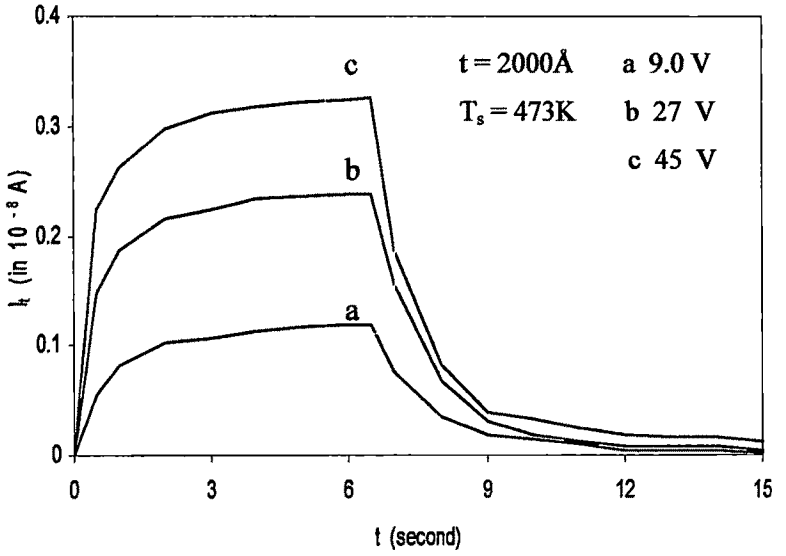

Figure 5.3(d) Growth and decay of photocurrent, $I_{ph}(t)$, of a CdSe thin film grown at elevated T_s and illuminated by monochromatic light (725 nm).

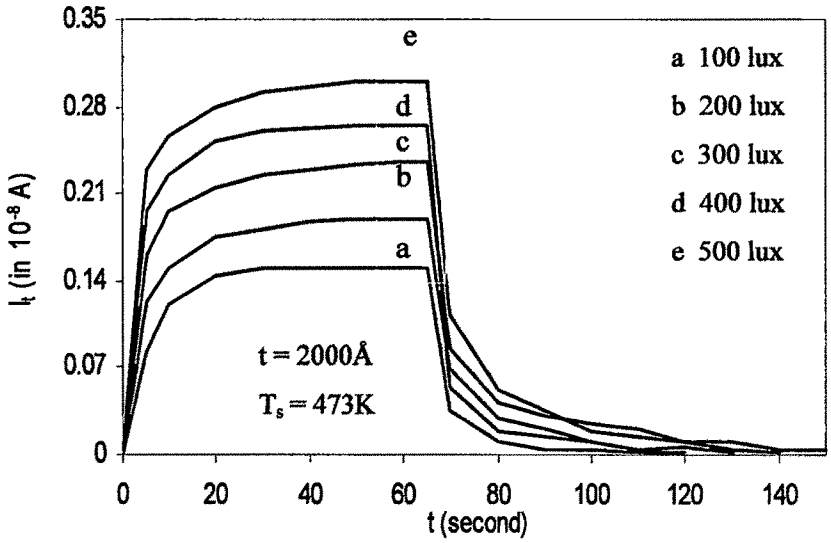

Figure 5.4(a) Growth and decay of photocurrent, $I_{ph}(t)$, of a CdSe thin film grown at elevated T_s and illuminated by white light.

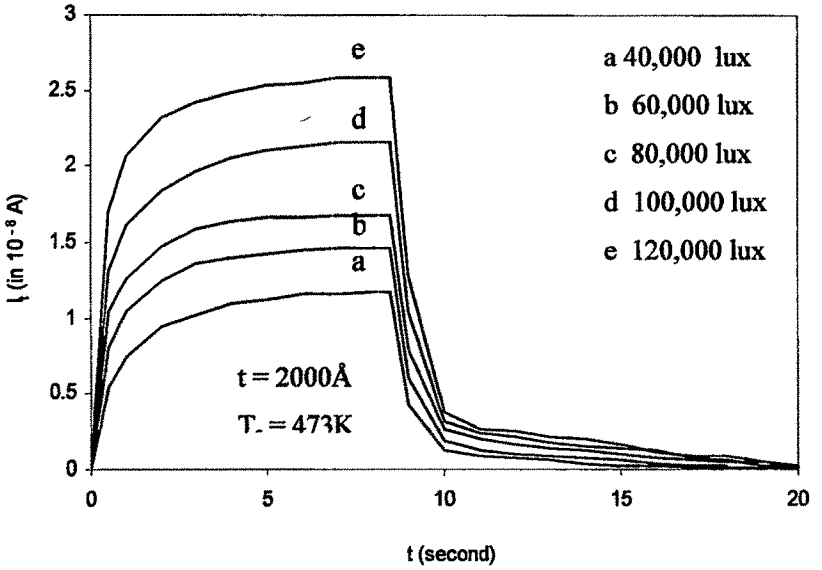

Figure 5.4(b) Growth and decay of photocurrent, $I_{ph}(t)$, of a CdSe thin film grown at elevated T_s and illuminated by white light

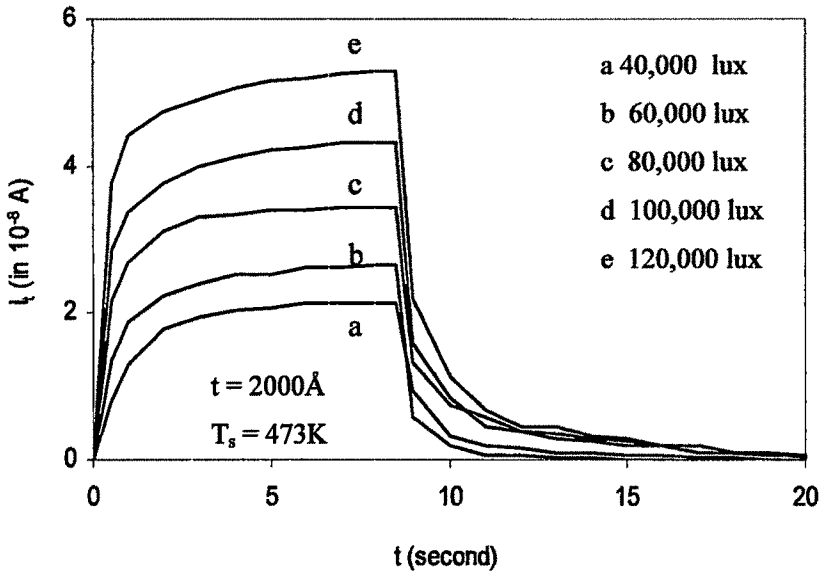

Figure 5.4(c) Growth and Decay of photocurrent, $I_{ph}(t)$, of a CdSe thin film grown at elevated T_s , illuminated by white light, at an ambient temperature 333K.

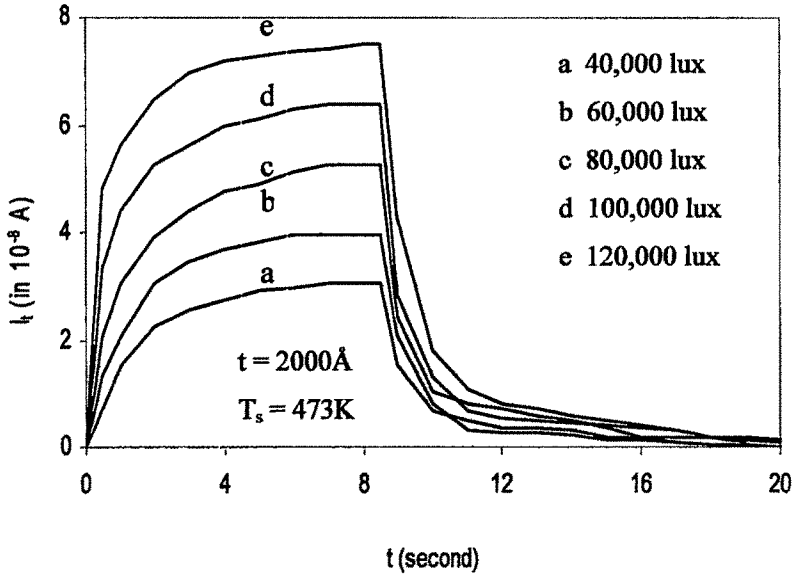

Figure 5.4(d) Growth and decay of photocurrent, $I_{ph}(t)$, of a CdSe thin film grown at elevated T_s , illuminated by white light, at an ambient temperature 363K

At high illumination the generation rate of free carriers is much greater than the number of trapped carriers and so electrons recombine with holes without significantly involving trapping processes /25/. The rise time and decay time are also found to be dependent on the applied bias [Fig 5.3(d)] and ambient temperature [Fig 5.4(c) & Fig 5.4(d)].

The higher value of rise and decay time obtained in the films indicate large ratios of concentrations of filled traps and free carriers due to illumination in the equation for time constant of rise and decay of photocurrent /26/,

$$\tau_{o(n)} = \{1+ (n_t/n)\}\tau_n \qquad (5.10a)$$

$$\tau_{o(p)} = \{1+ (p_t/p)\}\tau_p \qquad (5.10b)$$

where n_t or p_t is the electron and hole density in the traps, n or p is the free carrier density and τ_n or τ_p is the electron and hole life time. The slow release of trapped charge carriers increases the decay time. The presence of deep traps is also evident from this fact.

5.3.4 Trap depth analysis

Different optoelectronic properties of polycrystalline CdSe thin films are greatly influenced by both native and foreign imperfections. Native defects such as traps can cause a considerable change in electrical as well as the optical properties of the semiconductor thin films /27,28/. These defects characterize the electronic properties of the material because they generally give rise to charged centers acting as donors or acceptors /29/.

Actually trapping is a fundamental process for energy storage in almost all electronically active solids as well as thin films. This storage is accompanied by the spatial localization of an excited electron or hole, in such a way that the electron or hole is prohibited from moving freely through the crystal unless supplied with thermal or optical energy. When the trapped electron or hole is released, it is free to move until the captured electrons and holes are detained in a restricted volume, called traps /30,31/

The trap depths were calculated by using the following simple decay law

$$I_t = I_o \exp(-pt) \qquad (5.11)$$

where p is the probability of escape of an electron from the trap per second and is given by /32/

$$p = S \exp(-E / kT) \tag{5.12}$$

where E is the trap depth for electrons below the bottom of the conduction band or top of the valanced band, k is the Boltzmann constant, T is the ambient temperature in K , I_0 is the photocurrent at the termination of illumination, I_t is the photocurrent at any subsequent time t after the termination of illumination and S is the frequency factor defined in terms of number per second that the quanta from the lattice vibrations (phonons) attempt to eject the electron from the trap, multiplied by the probability of transition of the ejected electron to the conduction band /33/.

Using the two relations (5.11) and (5.12), the expression for trap depth is given by

$$E = kT [\ln S - \ln \{ \ln (I_0/I_t) / t\}] \tag{5.13}$$

The probability of an electron escaping from a trap of depth E and cross-section for its capture S_t , at a temperature T, is given by /34/

$$p = N_{eff} v_{th} S_t \exp(-E/kT) \tag{5.14}$$

where N_{eff} is the effective density of states in the conduction band and v_{th} is the thermal velocity of the electrons. Here the product $N_{eff} v_{th} S_t$ represents the frequency factor S.

For finding S, the values of these three parameters N_{eff}, v_{th}, and S_t were calculated separately. N_{eff} was calculated from the conductivity data by using the relation, $n = \sigma/e\mu^*$ /35/, where σ is the conductivity evaluated from the experimental data of the photocurrent I_0. In this case, it is assumed that at comparatively low temperatures, the number of occupied energy levels in the conduction band i.e. n is identical with N_{eff}. μ is the mobility of the electrons in CdSe sample whose value was taken to be 580 $cm^2 V^{-1} sec^{-1}$ /36/. The thermal velocity v_{th} of an electron was calculated at different ambient temperatures by using the relation,

$$v_{th} = (2kT / m^*)^{1/2} \tag{5.15}$$

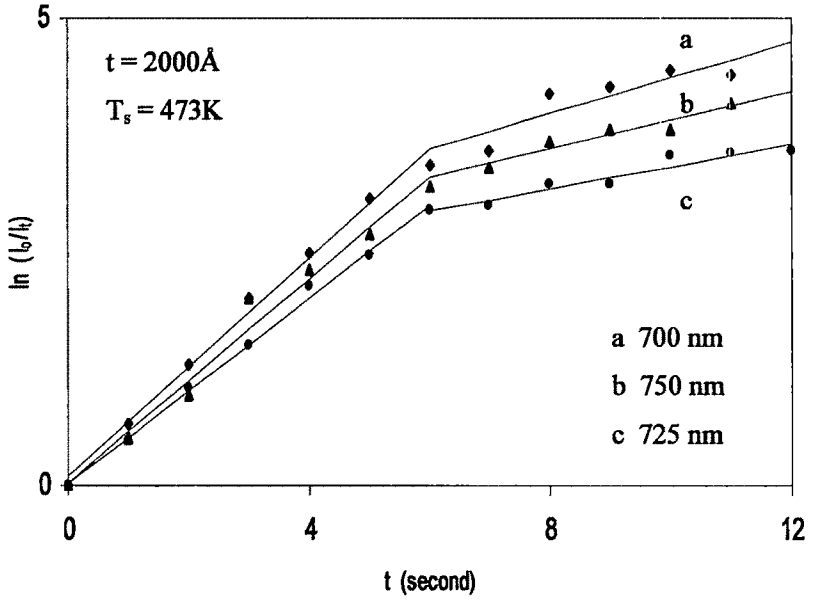

Figure 5.5(a) $\ln(I_0/I_t)$ versus time plot of a CdSe thin film grown at elevated T_s and illuminated by monochromatic light.

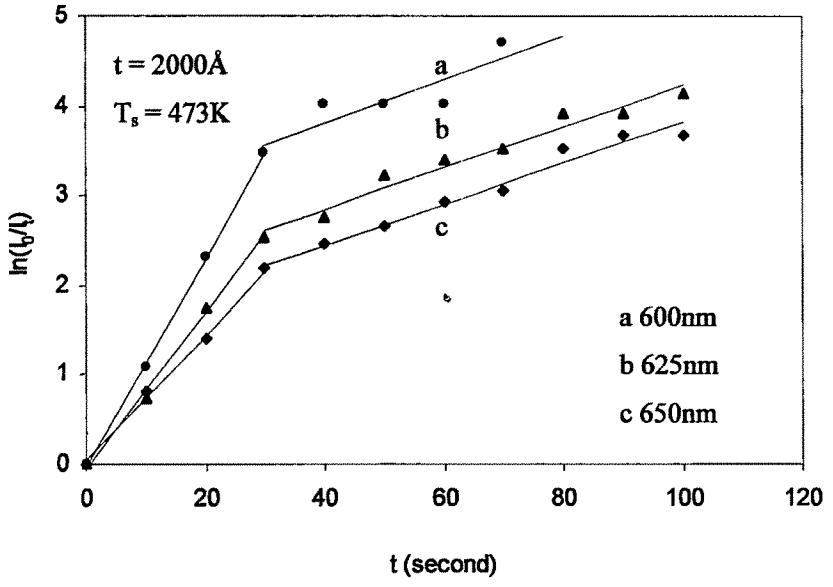

Figure 5.5(b) $\ln(I_0/I_t)$ versus time plot of a CdSe thin film grown at elevated T_s and illuminated by monochromatic light.

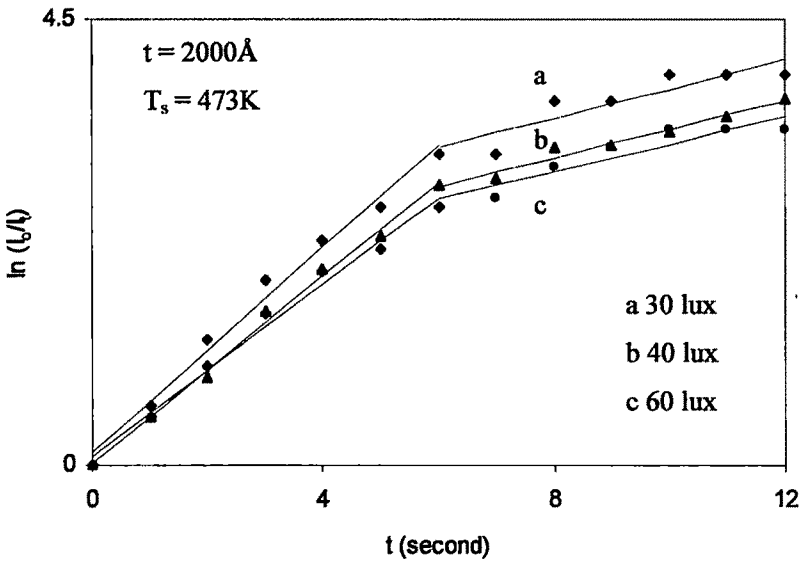

Figure 5.5(c) $\ln(I_0/I_t)$ versus time plot of a CdSe thin film grown at elevated T_s and illuminated by monochromatic light (725nm).

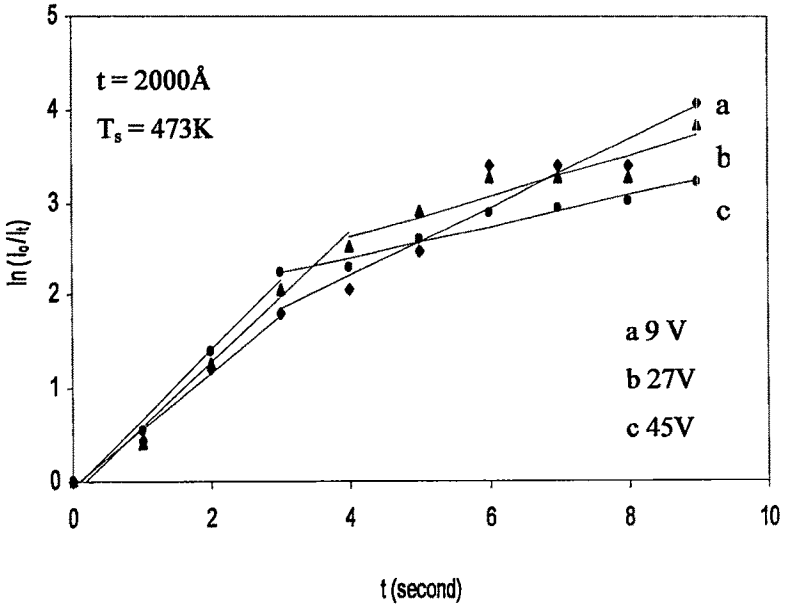

Figure 5.5(d) $\ln(I_0/I_t)$ versus time plot of a CdSe thin film grown at elevated T_s under different bias voltages and illuminated by monochromatic light (725nm).

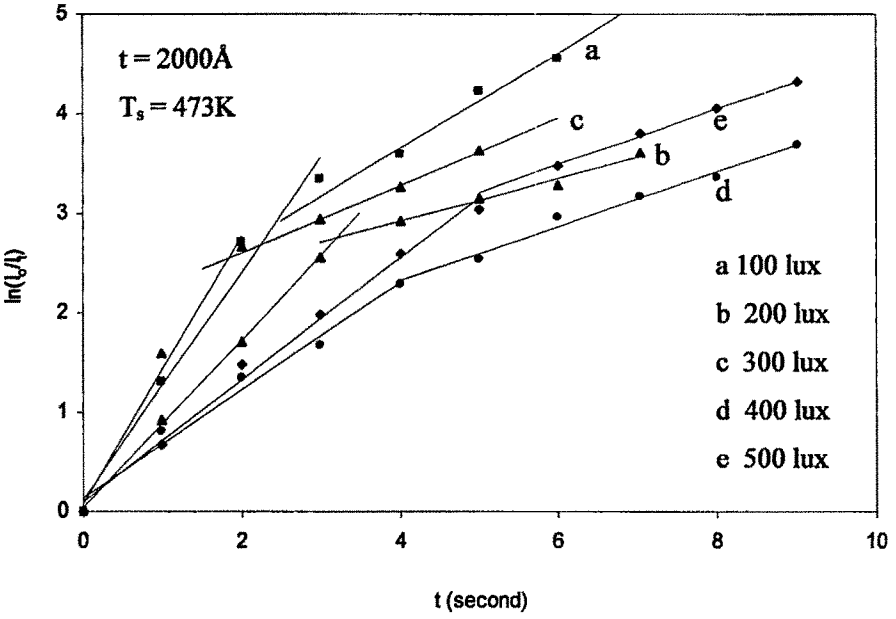

Figure 5.6(a) $\ln(I_0/I_t)$ versus time plot of a CdSe thin film grown at elevated T_s and illuminated by white light.

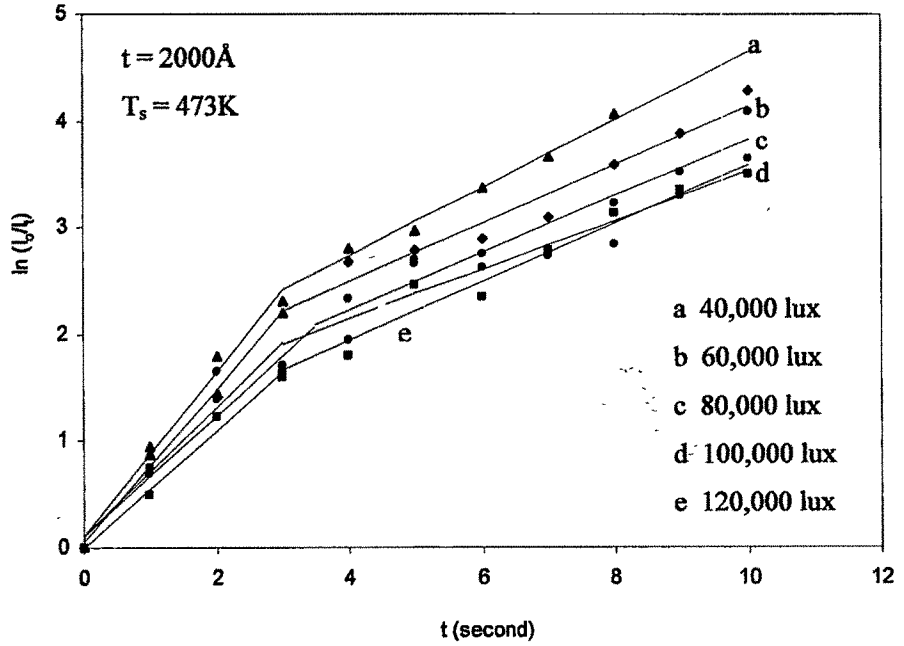

Figure 5.6(b) $\ln(I_0/I_t)$ versus time plot of a CdSe thin film grown at elevated T_s and illuminated by white light.

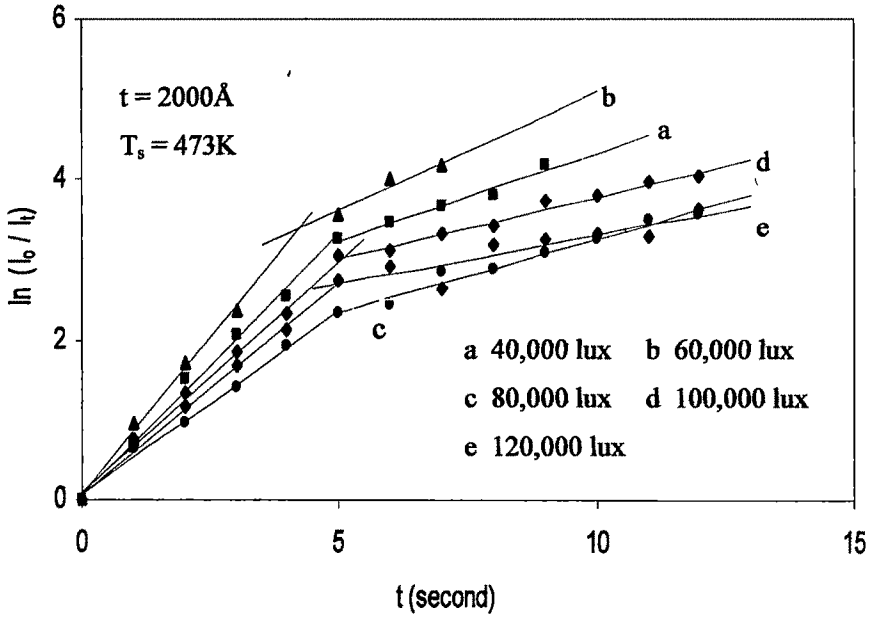

Figure 5.6(c) $\ln(I_0/I_t)$ versus time plot of a CdSe thin film grown at elevated T_s and illuminated by white light, at an ambient temperature 333K.

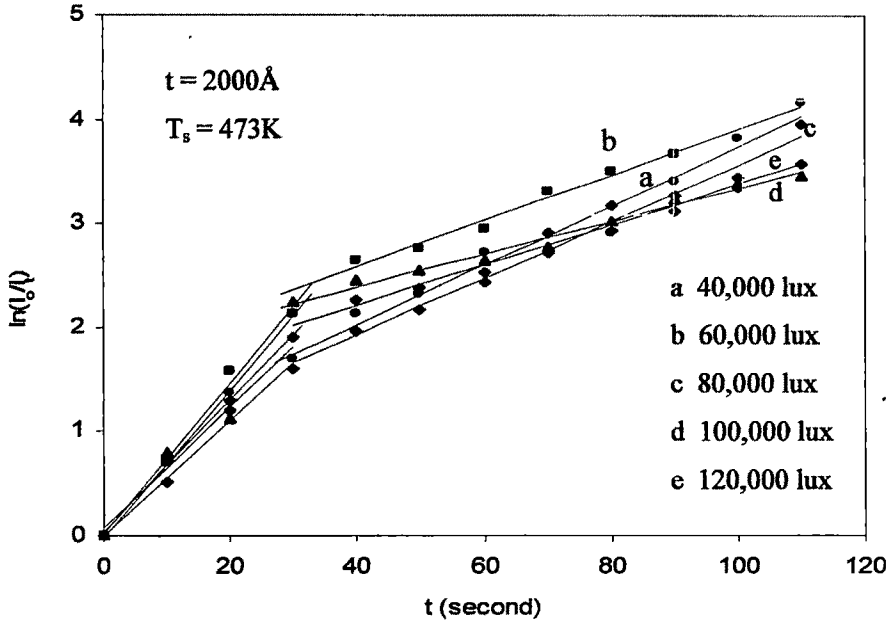

Figure 5.6(d) $\ln(I_0/I_t)$ versus time plot of a CdSe thin film grown at elevated T_s and illuminated by white light, at an ambient temperature 363K.

Table 5.1(a) Calculated values of σ, N_{eff}, S and E of a CdSe thin film (t = 2000Å, T_s = 473K) under different monochromatic illuminations

Illumination		σ $(\Omega\ cm)^{-1}$	N_{eff} (cm^{-3})	S (sec^{-1})	E (eV)	
Intensity (lux)	λ (nm)	in 10^{-5}	in 10^{10}	in 10^{6}	E_1	E_2
50	700	0.41	4.50	2.69	0.39	0.42
	750	0.35	3.77	2.25	0.39	0.42
	725	0.43	4.63	2.76	0.40	0.43
30	725	0.30	3.30	1.97	0.39	0.42
40		0.39	4.28	2.55	0.40	0.43
60		0.57	6.21	3.71	0.41	0.43

Table 5.1(b) Calculated values of σ, N_{eff}, S and E of a CdSe film (t = 2000Å, T_s = 473K) under different monochromatic illuminations and applied bias conditions.

Applied bias (volt)	Illumination λ (nm)	σ $(\Omega\ cm)^{-1}$ in 10^{-5}	N_{eff} (cm^{-3}) in 10^{10}	S (sec^{-1}) in 10^{6}	E (eV)	
					E_1	E_2
18	600	0.10	1.16	0.69	0.40	0.44
	625	0.09	1.06	0.63	0.40	0.44
	650	0.13	1.49	0.89	0.42	0.45
9	725	0.47	5.06	3.02	0.39	0.41
27		0.31	3.34	1.99	0.38	0.41
45		0.25	2.73	1.63	0.37	0.41

Table 5.2(a) Calculated values of σ, N_{eff}, S and E of a CdSe thin film (t = 2000Å, T_s = 473K) under different white light illuminations, at room temperature 300K.

Intensity of illumination (lux)	σ $(\Omega\ cm)^{-1}$ in 10^{-5}	N_{eff} (cm^{-3}) in 10^{10}	S (sec^{-1}) in 10^{6}	E (eV)	
				E_1	E_2
100	0.29	3.17	1.89	0.37	0.39
200	0.37	3.99	2.38	0.38	0.41
300	0.45	4.99	2.98	0.39	0.41
400	0.51	5.56	3.32	0.40	0.42
500	0.58	6.29	3.76	0.40	0.42

Table 5.2(b) Calculated values of σ, N_{eff}, S and E of a CdSe film (t = 2000Å, T_s = 473 K) under different white light illuminations, at room temperature 300K.

Intensity of illumination (lux)	σ $(\Omega\ cm)^{-1}$ in 10^{-5}	N_{eff} (cm^{-3}) in 10^{10}	S (sec^{-1}) in 10^{6}	E (eV)	
				E_1	E_2
40,000	2.28	24.58	14.69	0.43	0.45
60,000	2.84	30.66	18.33	0.44	0.46
80,000	3.27	35.30	21.11	0.45	0.47
100,000	4.19	45.18	27.01	0.45	0.48
120,000	5.03	54.24	32.43	0.46	0.48

Table 5.2(c) Calculated values of σ, N_{eff}, S and E of a CdSe film (t = 2000Å, T_s = 473 K) under different white light illuminations, at an ambient temperature 333K

Intensity of illumination (lux)	σ $(\Omega\ cm)^{-1}$ in 10^{-5}	N_{eff} (cm^{-3}) in 10^{10}	S (sec^{-1}) in 10^{6}	E (eV)	
				E_1	E_2
40,000	4.19	45.15	28.86	0.51	0.54
60,000	5.19	55.93	35.76	0.52	0.54
80,000	6.70	72.26	46.20	0.53	0.55
100,000	8.38	90.32	57.75	0.55	0.56
120,000	10.35	111.53	71.31	0.55	0.57

Table 5.2(d) Calculated values of σ, N_{eff}, S and E of a CdSe film (t = 2000Å, T_s = 473 K) under different white light illuminations, at an ambient temperature 363K

Intensity of illumination (lux)	σ $(\Omega\ cm)^{-1}$ in 10^{-5}	N_{eff} (cm^{-3}) in 10^{10}	S (sec^{-1}) in 10^{6}	E (eV)	
				E_1	E_2
40,000	5.94	64.08	42.88	0.63	0.66
60,000	7.72	83.18	55.67	0.64	0.67
80,000	10.29	110.80	74.15	0.65	0.68
100,000	12.48	134.48	90.00	0.66	0.69
120,000	14.62	157.53	105.4	0.67	0.70

where m* is the effective mass of an electron which was taken to be $0.13m_e$ /37/. The capture cross-section is given by

$$S_t = \pi r^2 \tag{5.16}$$

where r is the radius of the capture center. It was evaluated by putting the Coulomb energy of interaction of an electron with the corresponding trap equal to the thermal energy of the electron at temperature T /38/. i.e.

$$e^2 / r\varepsilon = kT \tag{5.17}$$

where ε is the dielectric constant of CdSe sample whose value is taken to be 5.76 /39/. Using (5.17) in (5.16) the relation for capture cross section is given by

$$S_t = \pi e^4 / k^2 T^2 \varepsilon^2 \tag{5.18}$$

At 300 K, $S_t \approx 10^{-10}/\varepsilon^2$ cm^2 /40/

Using the relation $S = N_{eff}\, v_{th}\, S_t$, the frequency factor, S, at different ambient conditions were evaluated. The different calculated values of N_{eff} and S are shown in the Table 5.1(a, b) and Table 5.2(a to d).

From these tables, it is seen that there is a gradual increase in the value of S with ambient temperature as well as with intensity of illumination. Using values of p, evaluated from the slopes of $\ln(I_0/I_t)$ versus time plots, under different conditions, shown in Figs 5.5(a to d) and Figs 5.6(a to d), and S, in the relation (5.13), the trap depths at different ambient conditions were calculated. The different values of trap depths are also systematically presented in the Table 5.1(a, b) and Table 5.2(a to d).

From the Figs 5.5(a to d) and Figs 5.6(a to d), it is observed that there exist two different slopes in $\ln(I_0/I_t)$ versus time plots, which indicates the existence of two distinct trap levels, E_1 and E_2, at any ambient temperature. From these evaluated values of E, it is seen that there is a quasi-continuous distribution of trap levels below the conduction band /41/. It may be noted that photocurrent in these thin films was found to obey a sub-linear relation with the intensity of illumination which could be explained on the basis of defect controlled photoconductivity mechanism /42/.

CdSe thin film photoconductors contain traps with depths distributed over a range and form of this distribution determines the set of decay curve /43/. Shortly after the start of illumination an equilibrium is established when the rate of supply of electrons to the traps is equal to the rate of escape and the extent to which traps are filled is therefore depends on their depth energy E. Traps with large E becomes almost completely filled because the rate of escape of electrons from these traps is small. Shallow traps are partly filled because the rate of escape of electron from these traps is appreciable. When the exciting illumination is cut off the electrons continue to escape from the traps and produce slow decay of photocurrent. The shape of the decay curve depends upon the intensity of illuminating radiations. If the intensity of illuminating radiation is increased, more numbers of shallow trapped electrons as well as deep trapped electrons takes part in the decay process.

The depth E, which a trap required to posses in order that an electron may be trapped in it for time, varies with depth of trap. Hence the number of traps in which an electron spends a mean time, t, will vary with temperature and therefore I_t varies with temperature. Fig 5.7(a) and Fig 5.7(b) show the variation of trap energy with temperature. It is clear from the figures that trap depths E_1 and E_2 are not single valued but varies over a range with temperature.

5.3.5 Mobility activation in CdSe thin films

The effect of mobility of polycrystalline semiconductor in dark as well as under illumination, has been extensively studied by different workers /44, 45/. In the study of mobility activation process of CdSe thin films, the effect of grain boundaries on the photoconductivity has been considered, which produces stress on the below band gap optical process.

As already mentioned that thin films of CdSe grown at elevated T_s are of polycrystalline nature having grains of different sizes. These films have some built in potential barriers, ϕ_b at the grain boundaries and this grain boundary potential can be expressed by the equation (4.21).

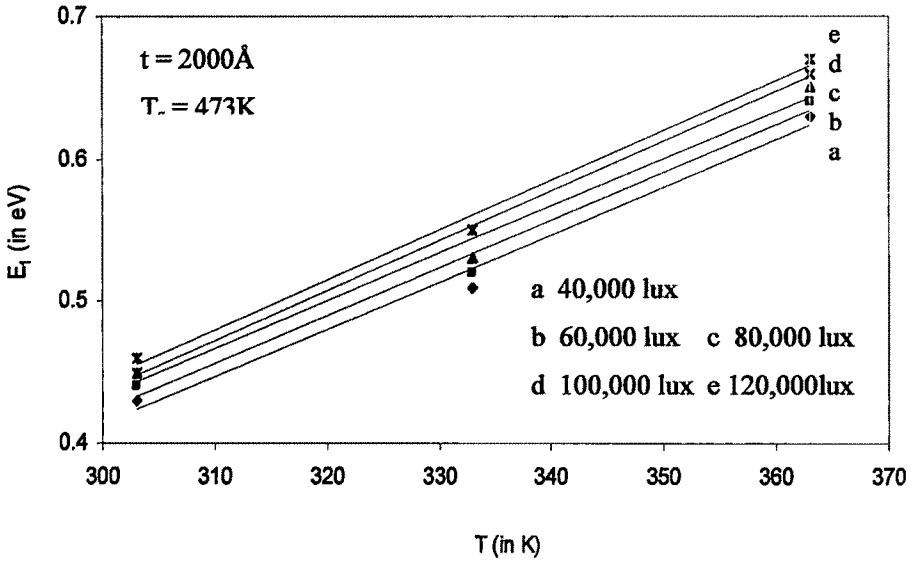

Figure 5.7(a) Plot of trap depths (E_1) versus ambient temperature (T) at different intensity of illuminations of a CdSe thin film grown at elevated T_s.

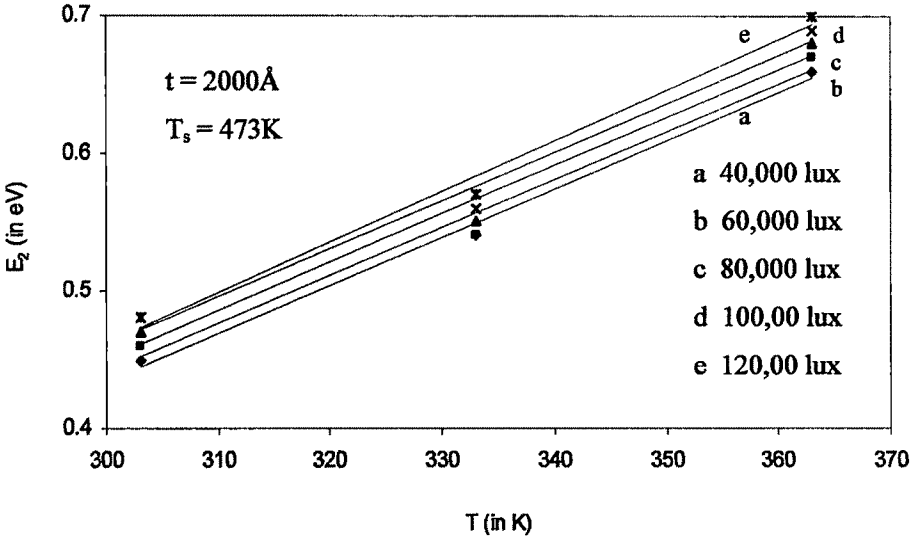

Figure 5.7(b) Plot of trap depths (E_2) versus ambient temperature (T) at different intensity of illuminations of a CdSe thin film grown at elevated T_s.

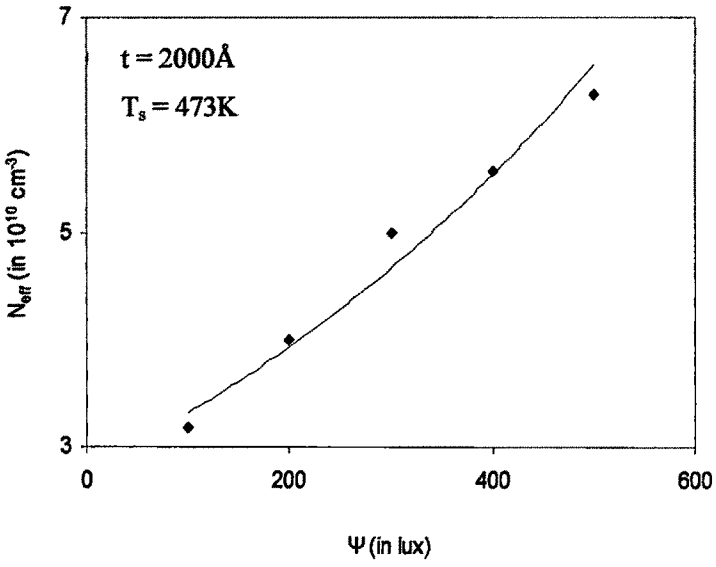

Figure 5.8(a) Density of states (N_{eff}) versus intensity of illumination (Ψ) at room temperature of a CdSe thin film grown at elevated T_s.

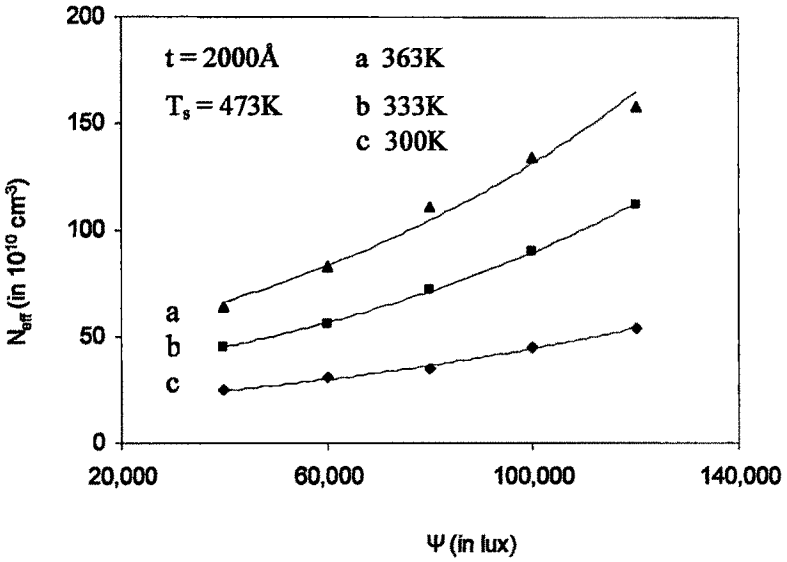

Figure 5.8(b) Density of states (N_{eff}) versus intensity of illumination (Ψ) at different ambient temperatures of a CdSe thin film grown at elevated T_s.

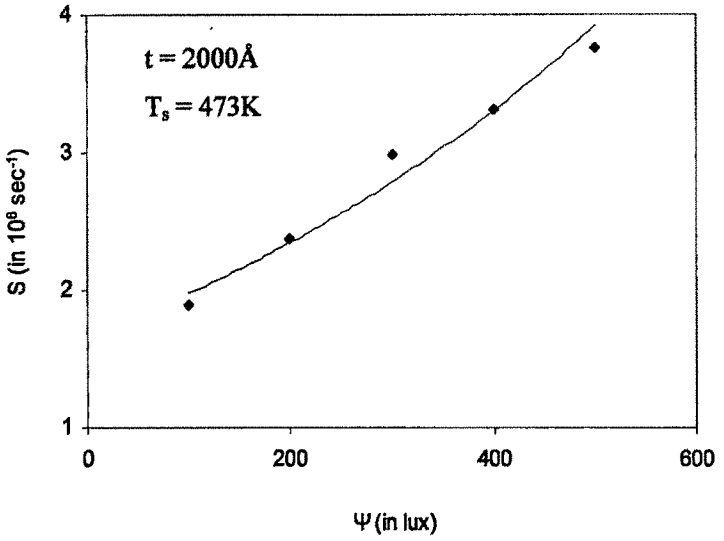

Figure 5.9(a) Frequency factor (S) versus intensity of illumination (Ψ) at room temperature of a CdSe thin film grown at elevated T_s.

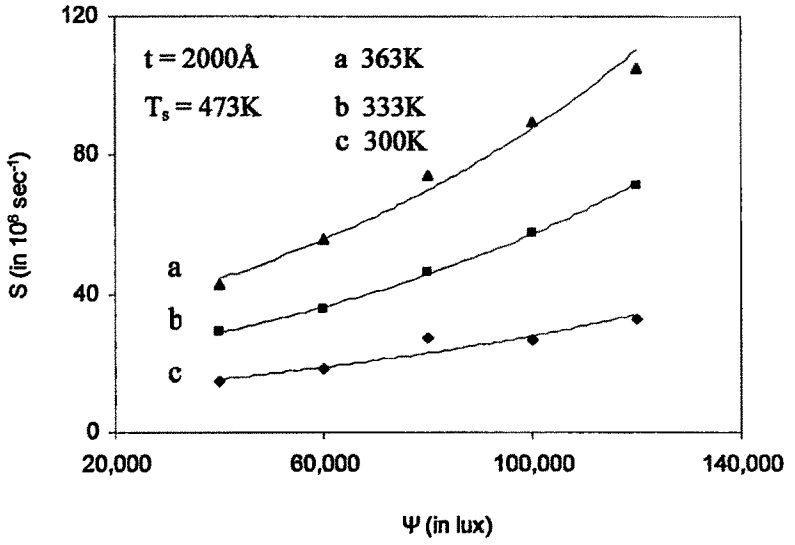

Figure 5.9(b) Frequency factor (S) versus intensity of illumination (Ψ) at different ambient temperature of a CdSe thin film grown at elevated T_s.

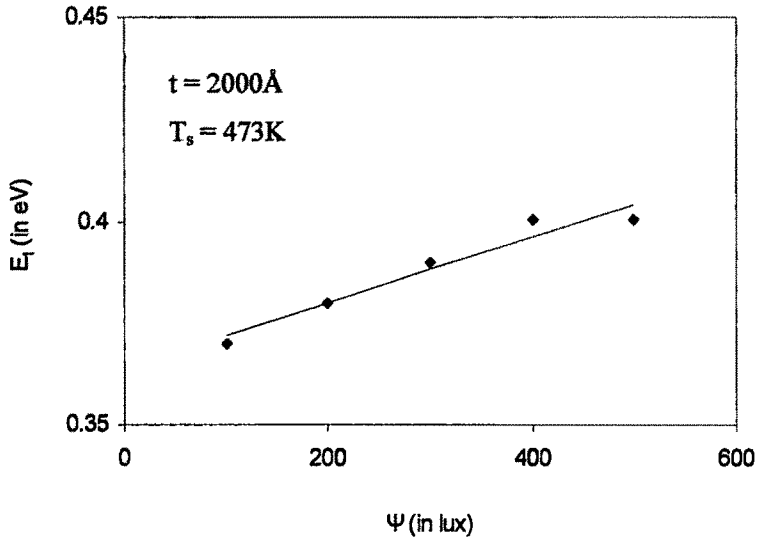

Figure 5.10(a) Trap depth (E_1) versus intensity of illumination (Ψ) at room temperature of a CdSe thin film grown at elevated T_s.

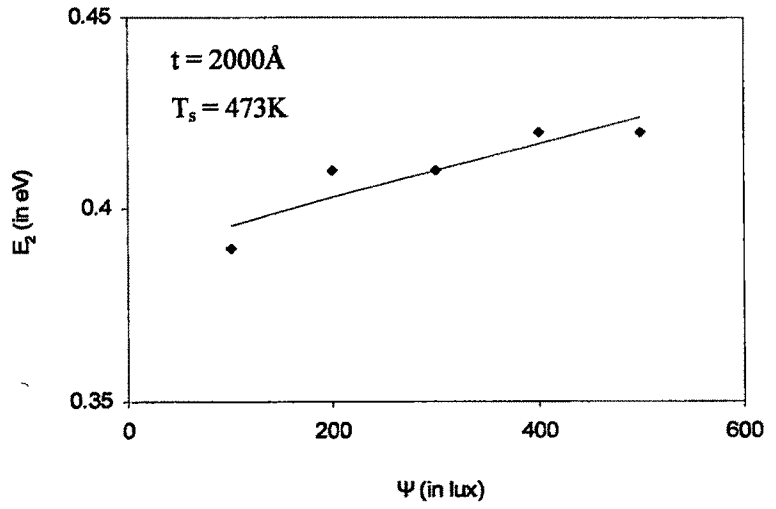

Figure 5.10(b) Trap depth (E_2) versus intensity of illumination (Ψ) at room temperature of a CdSe thin film grown at elevated T_s.

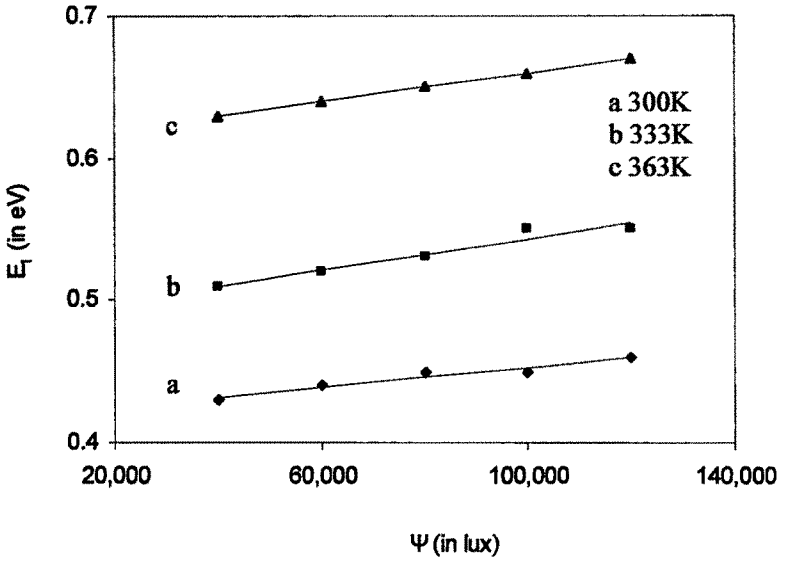

Figure 5.11(a) Trap depth (E_1) versus intensity of illumination (Ψ) at different ambient temperature of a CdSe thin film grown at elevated $T_s = 473K$.

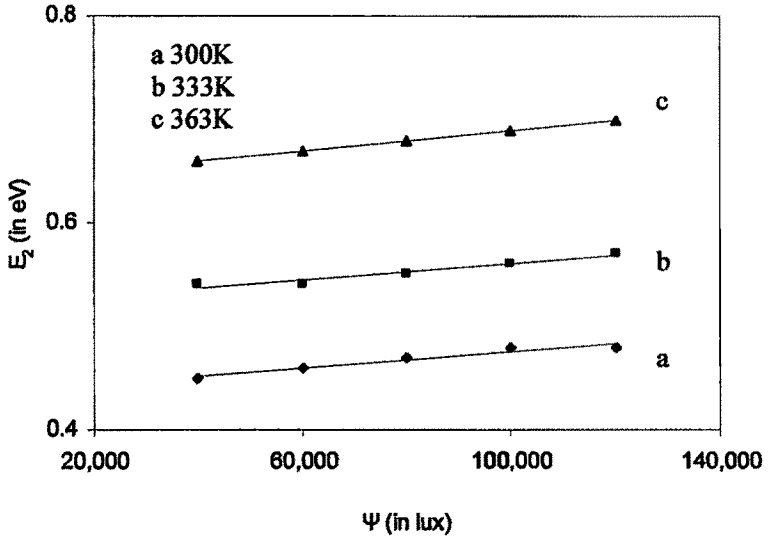

Figure 5.11(b) Trap depth (E_2) versus intensity of illumination (Ψ) at different ambient temperature of a CdSe thin film grown at elevated $T_s = 473K$.

Due to the absorption of illuminating radiation (ψ) free electron hole pairs are generated. The photogenerated electrons and holes which are in excess to the thermal equilibrium number density of carriers are responsible for photoconduction process. One part of the photogenerated carriers recombine with respective opposite charges localized at grain boundary depletion regions, thereby reduces the grain boundary potential barriers, ϕ_b and the rest takes part in the photoconduction process. As a result of reduction of, ϕ_b the effective mobility of the carriers increases. This process is known as barrier modulation. The effective mobility μ^* is given by the equation (4.12). Due to the increase in μ^* also, the conductivity of the sample increases.

Hence the increase in photoconductivity is due to two contributors viz one from the resultant increase in the photogenerated carriers and the other from the increase in the effective mobility. Thus the photoconductivity is given by

$$\sigma = N_{eff}\, q\, \mu^*. \tag{5.19}$$

where N_{eff} is the effective density of states in the conduction band under illumination which is assumed to be the numbers of occupied energy levels n, in the conduction band by the electrons. Thus N_{eff} can be written as

$$N_{eff} = 2\,(2\pi kT/h^2)^{3/2}\,(m_e^* m_h^*)^{3/4} \exp(-E_g/kT) \tag{5.20}$$

Therefore

$$\begin{aligned}\sigma &= 2\,(2\pi kT/h^2)^{3/2}\,(m_e^* m_h^*)^{3/4} \exp(-E_g/kT)\; q\, \mu_o \exp(-q\Phi_b/kT_o) \\ &= C \exp(-q\Phi_b/kT_o)\end{aligned} \tag{5.21}$$

where $C = 2\,(2\pi kT/h^2)^{3/2}\,(m_e^* m_h^*)^{3/4} \exp(-E_g/kT)\; q\, \mu_o$

From equation (5.21) one can write

$$\ln \sigma = \ln C + (-q\Phi_b / kT_o) \tag{5.22}$$

It can be seen from Fig 5.8(a) and Fig 5.8(b), the values of N_{eff} ($N_{eff} = n$) calculated from experimental σ data bear an exponential relation with the incident intensity of illumination, ψ. This is in good agreement with equation (5.21). It may noted that $\ln N_{eff}$

$\propto \psi$. This implies that ϕ_b is inversely proportional to ψ, which justifies the barrier modulation process.

The traps may be emptied by the absorption of optical radiation of different intensity as well as by the utilization of thermal energy. So the trap depths can be calculated from the spectrum of photoconductivity decay curve. As already mentioned $S = N_{eff} v_{th} S_t$, where N_{eff} is the density of states, v_{th} is the thermal velocity of the electrons, S_t is the capture cross section of the electron at any trap level. With the increase in intensity of illumination, N_{eff} increases exponentially [Fig 5.8(a) & Fig 5.8(b)] whereas v_{th} and S_t remain constant. So the frequency factor, S, also increases exponentially with illumination as shown in Fig 5.9(a) and Fig 5.9(b). It can be noted that $\ln S \propto \psi$, hence

$$\ln S = C\psi \tag{5.23}$$

where C is the proportionality constant. So, S, which is directly proportional to N_{eff} (or n), becomes the main contributory term of the trap energy. The ratio I_0/I_t is nearly constant at any illumination level. Thus the term $\ln\{\ln(I_0/I_t)/t\}$ in equation (5.13) has a little contribution in the trap energy. Hence the dependence of trap energy, E, is basically determined by the term lnS. Therefore E, is expected to be proportional to ψ. This is seen to be justified by the plots E_1 and E_2 vs ψ as shown in Figs 5.10(a, b) and Figs 5.11(a, b).

5.3.6 Study of optical properties

Optical properties of thin films have been studied extensively primarily because of their applications in various optical and electro-optical devices. Generally there is often a considerable deviation of optical parameters in thin films from their bulk counterparts /46/. Interaction of electromagnetic waves with solids leads to their optical properties and are manifested in optical frequencies. After the incidence of a ray of light on a sample it is partly reflected and partly transmitted. The phenomenon like scattering, polarization and absorption may also be associated with it. Out of these transmission and absorption occurs inside the medium of the sample. The path of a ray of light in the transmitted medium deviates from that of the incident one and the deviation depends on

the nature of the materials in the two concerned media. The denser is the second medium, relative to the first, more will be the deviation.

When the process is considered in case of a thin film, at least two interfaces are to be taken into account namely air/film and film/air on the other side of the incident beam and more often a third interface viz film/substrate. The study of optical absorbance and transmittance provide a simple means for the determination of absorption edge, optical energy band gap, optical transitions which may be direct or indirect, allowed or forbidden. It also provides information regarding the nature of the solid material. The interactions of electromagnetic waves with a thin film may cause several transitions in its band structure such as band to band, between sub bands or impurity levels and a band, transitions of free carriers within a band and also resonance due to lattice vibrations. These lead to the appearance of bands or absorption peak in the absorbance spectra. Therefore an indepth study of the absorption band spectra is likely to provide a wealth of information about electronic band structure of thin films.

Absorption of light by the thin films takes place broadly by two processes namely (i) by raising the electrons from the valence band to the conduction band and (ii) by exciting the lattice vibrations of the material. In case of semiconductors the bound electrons in the valence band contribute to the optical process. As a part of the present investigations the transmittance and absorbance spectra of CdSe thin films have been taken at room temperature neglecting the contribution of thermal energy.

The CdSe thin film of thickness, t, has a complex refractive index, $n^* = n - ik$, where n is the refractive index and k is the extinction coefficient. The substrate is considered to be transparent ($k_s = 0$) and its refractive index is n_s. The thickness of the substrate is several orders of magnitude larger than, t.

The reflection coefficient, R_1 & R_2, and transmission coefficient, T_1 & T_2, for the two interfaces, air-film and film-substrate respectively, are given by the following expressions /47/

$$R_1 = \{(n-1)^2 + k^2\}/\{(n+1)^2 + k^2\} \qquad R_2 = \{(n-n_s)^2 + k^2\}/\{(n+n_s)^2 + k^2\}$$

$$= 1 - T_1 \qquad (5.24a) \qquad = 1 - T_2 \qquad (5.24b)$$

If the thickness of the film is constant, the transmission coefficient, T, and the reflection coefficient, R, due to the film, taking into account multiple reflections and interference effects, are given by /48/

$$T = T_1T_2\tau / \{1 - 2(R_1R_2)^{1/2}\tau\cos\Phi + R_1R_2\tau^2\} \quad (5.25a)$$

$$R = \{R_1 - 2(R_1R_2)^{1/2}\tau\cos\Phi + R_2\tau^2\} / \{1 - 2(R_1R_2)^{1/2}\tau\cos\Phi + R_1R_2\tau^2\} \quad (5.25b)$$

$$\text{where} \quad \tau = \exp(-\alpha t)$$

The absorption coefficient $\alpha = 4\pi k/\lambda$ and $\Phi = 4\pi nt/\lambda$. If $2nt = m\lambda$, where m is an integer (half integer), accordingly a maximum (minimum) in the transmission spectra is obtained.

The thermally deposited CdSe thin films show high transmittivity to visible light. Fig 5.12(a) and Fig 5.12(b) show the transmission and absorbance spectra of two heat treated CdSe thin film samples. The transmission coefficient of such films is found to be greater than that of untreated films. This fact is probably due to the increase in crystallite size. The inter-crystalline grain boundaries contain structural defects, impurities etc and these factors might influence the absorption process.

Fig 5.13(a) and Fig 5.13(b) illustrate the transmission curves for two CdSe films with relatively higher thickness grown at constant elevated T_s. The interference maximum and minimum due to multiple reflections on the film surface may be observed in case of Fig. 5.13(a). This shows that transmission coefficient strongly depends on the film structure, which is determined by the film thickness and its deposition conditions. For a good interference pattern smooth film surface is necessary. A very rough surface destroys the interference due to multiple reflections. The number of the interference fringes in the transmission curves is determined by the thickness of the film. For this comparatively thick film [Fig 5.13(a)], the refractive index, in the spectral domain of the medium and strong transmission, is calculated using the Swanpoel method /49/ of creating envelopes of the interference maxima and minima. Firstly an approximate value of refractive index (say n_1) is calculated using the expression /49/

$$n = [N + (N^2 - n_s^2)^{1/2}]^{1/2} \quad (5.26)$$

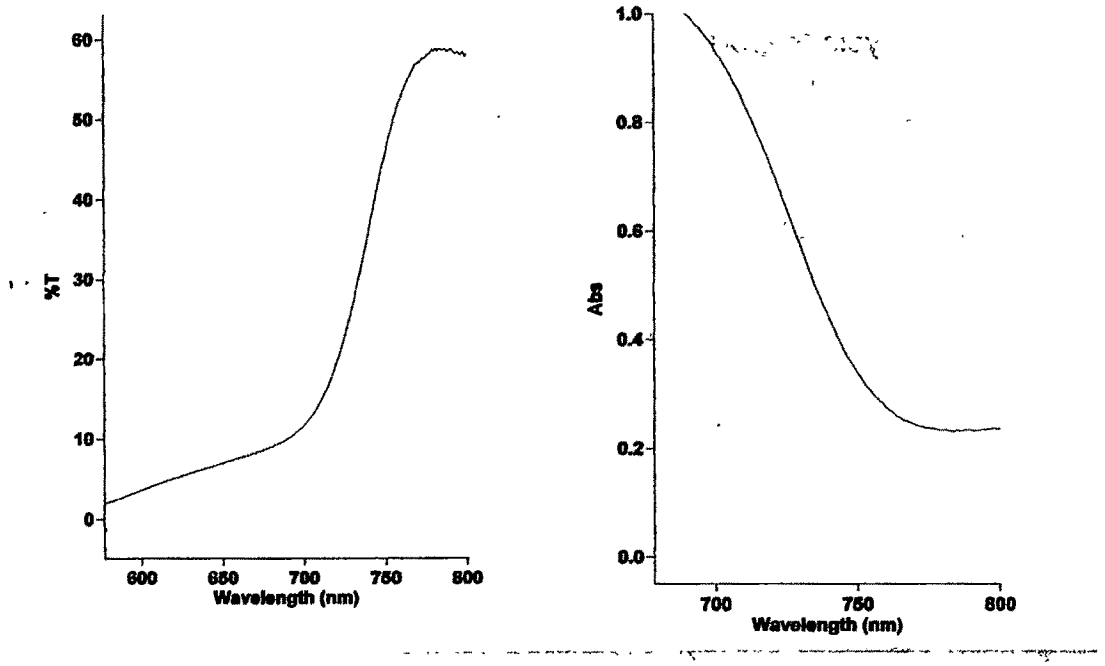

Figure 5.12(a) Transmission and absorbance spectra of a CdSe thin film (t = 2100Å) grown at elevated T_s = 523K.

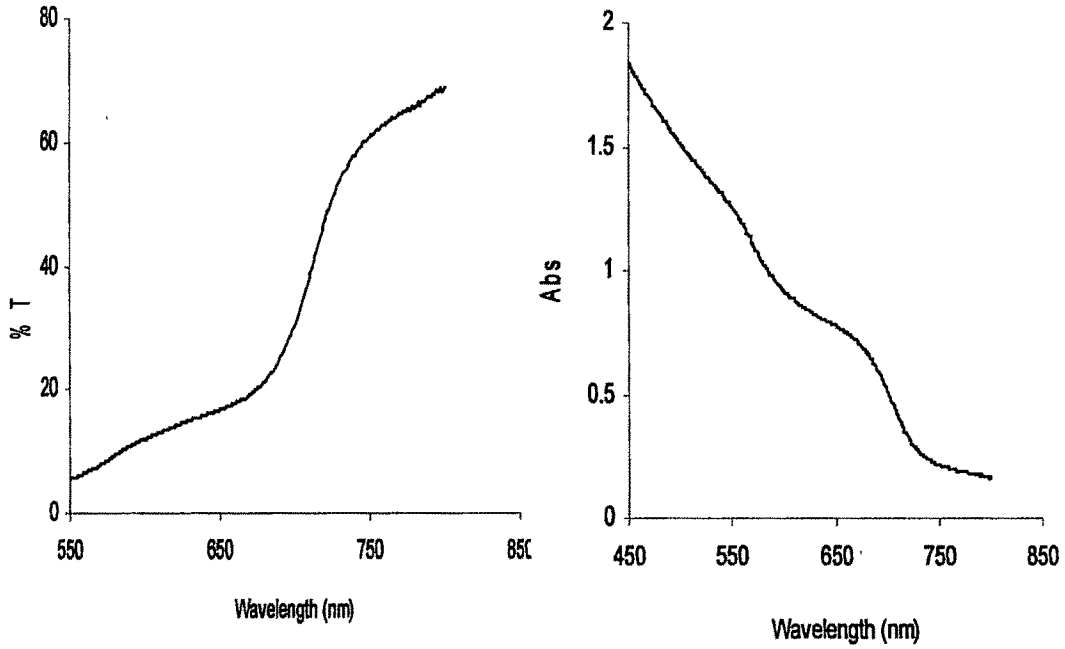

Figure 5.12(b) Transmission and absorbance spectra of a CdSe thin film (t = 2100Å) grown at elevated T_s = 473K

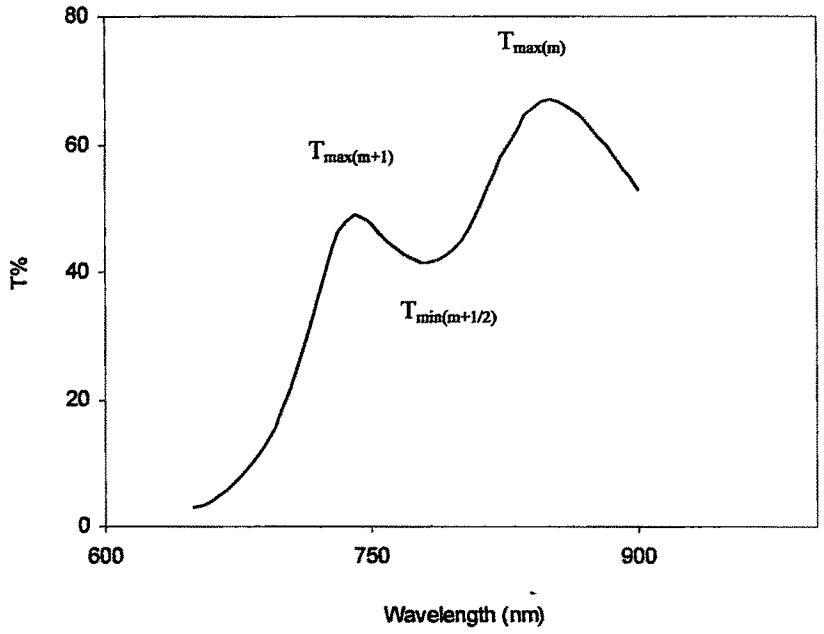

Figure 5.13(a) Transmission spectra of a CdSe thin film sample grown at elevated T_s = 523K and of thickness, t = 4950Å

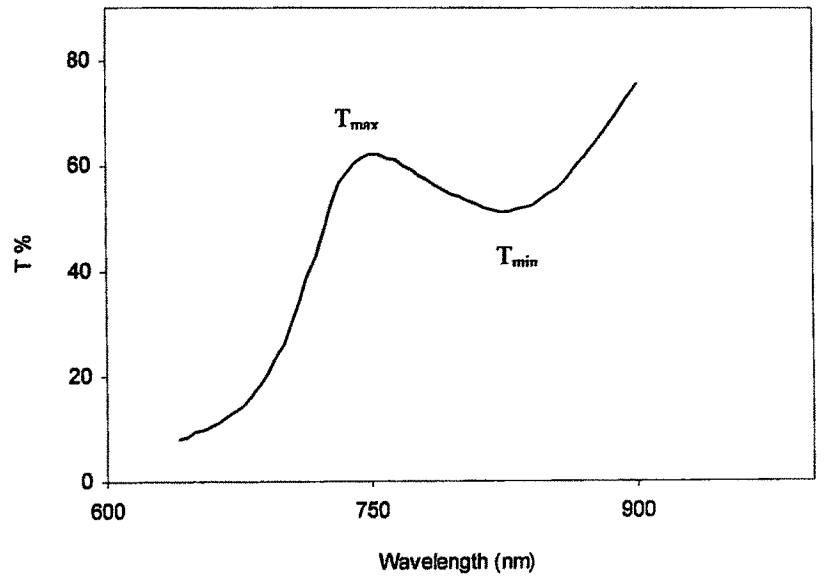

Figure 5.13(b) Transmission spectra of a CdSe thin film grown at elevated T_s = 523K and of thickness, t = 3860Å.

where $$N = \{2n_s(T_{max}-T_{min}) / T_{max}T_{min}\} + \{(2n^2_s+1) / 2\}$$

n_s is the refractive index of the substrate used and T_{max} & T_{min} are the transmission maximum and minimum at the same wavelength (λ).

With this value of the refractive index of the film, the 'order' m of the different extremes of the transmission curve is determined with the help of the equation for interference fringes

$$2nt = m\lambda \tag{5.27}$$

In this case thickness of the film, t, was known. The values of m are then approximated to the close integer (for maxima) or half integer (for minima) m_0 /50/. These values of m_0 are used to determine the new value of the refractive index, n, from the relation (5.27). In the interference free zone the refractive index were obtained by extrapolation of the refractive index obtained in the interference zone using Cauchy dispersion relation

$$n = A + B/\lambda^2 \tag{5.28}$$

Near the absorption edge the absorption coefficient can be calculated using the expression /51/

$$\alpha = 1/t \ln (1/T) \tag{5.29a}$$

where T is the transmittance. The extinction coefficient, k, is estimated from the value of α and λ using the formula

$$k = \alpha\lambda/4\pi \tag{5.29b}$$

Table 5.3 summarizes the calculated values of n, α and k of the typical thick CdSe thin film (t = 4950Å) at selected wave lengths in the interference region. Fig 5.14(a) shows the refractive index n versus $1/\lambda^2$ plot for the same film whereas Fig 5.14(b) and Fig 5.14(c) illustrates the dependence of refractive index and extinction coefficient on wavelength respectively.

The fundamental absorption may be due to either allowed direct transitions described by the relation /52/,

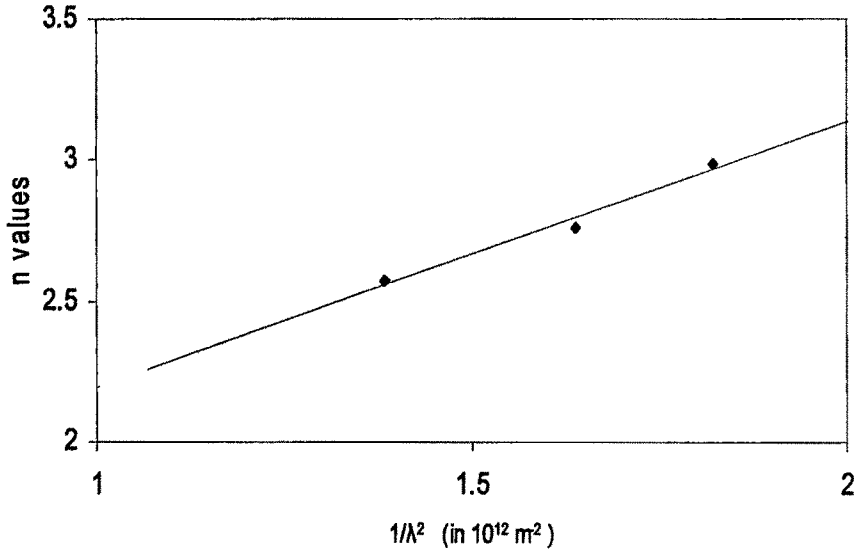

Figure 5.14(a) n versus $1/\lambda^2$ plot of a CdSe thin film of thickness t = 4950Å, T_s = 573K.

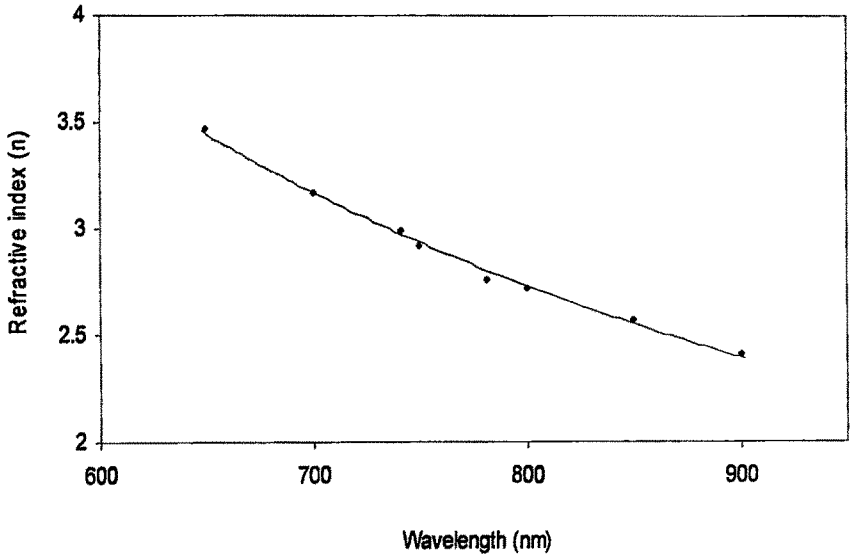

Figure 5.14(b) Variation of refractive index (n) with wavelength of a CdSe thin film of t = 4950Å, T_s = 573K.

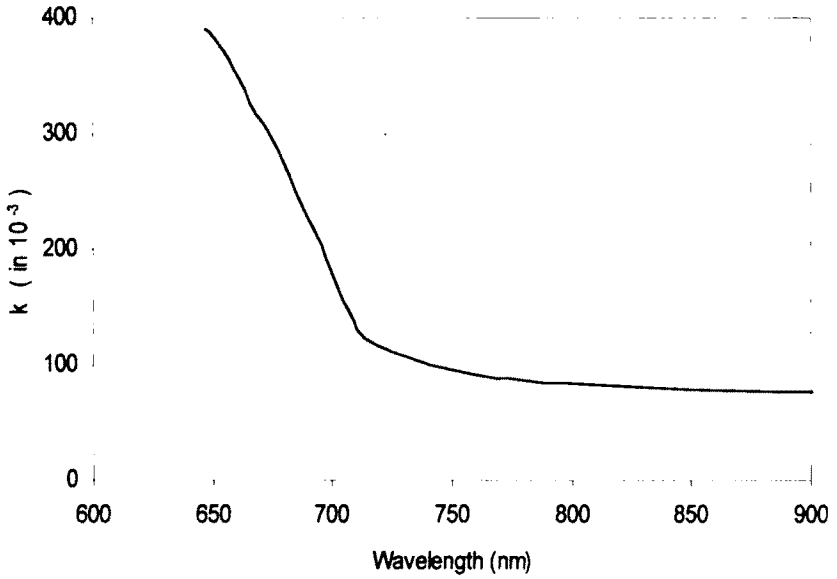

Figure 5.14(c) Variation of extinction coefficient (k) with wavelength of a CdSe thin film of t = 4950Å, T_s = 573K.

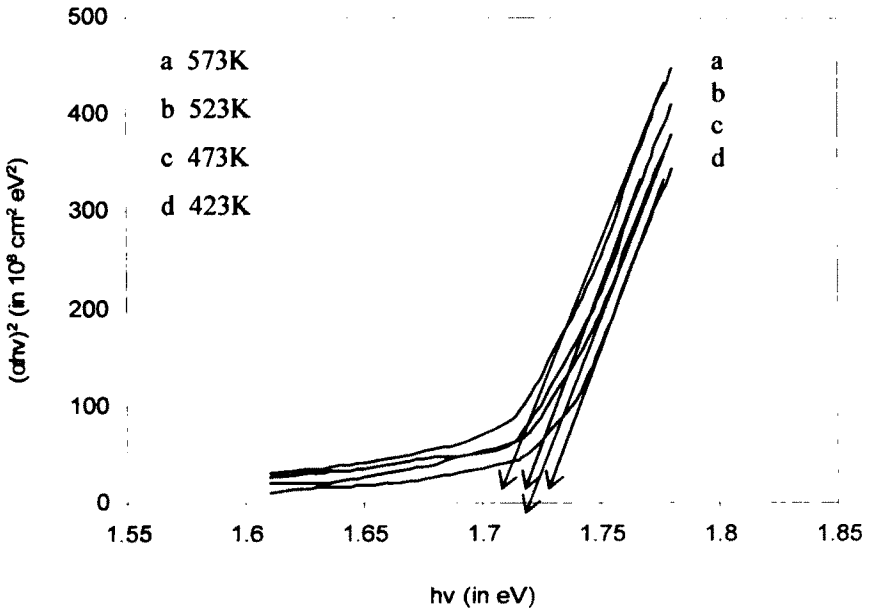

Figure 5.15(a) The $(\alpha h\nu)^2$ vs photon energy hν plots of CdSe thin films of constant thickness t = 2000Å and grown at different elevated T_s

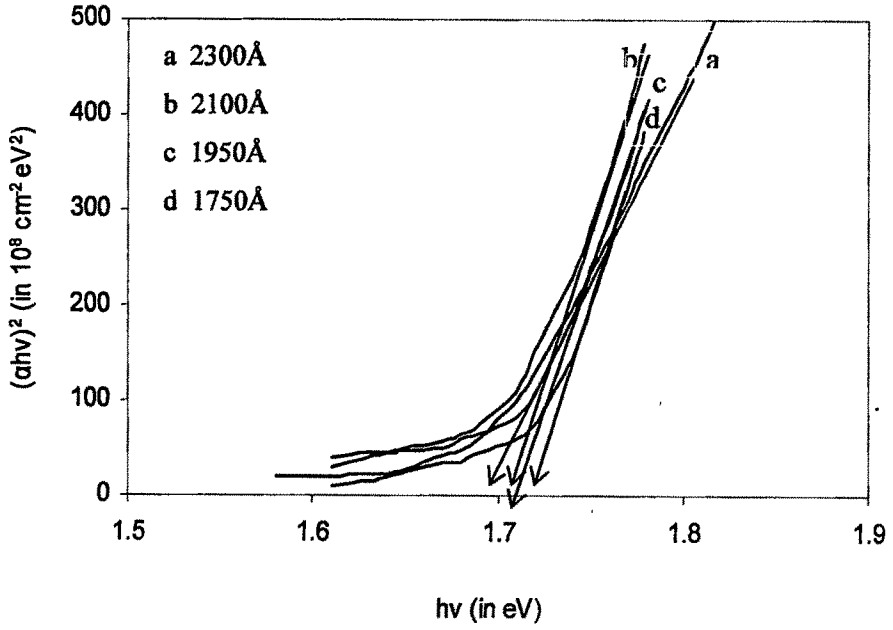

Figure 5.15(b) The $(\alpha h\nu)^2$ vs photon energy hν plots for a few CdSe films of different thickness and grown at constant elevated $T_s = 473K$.

Table 5.3 Values of refractive index, n, absorption coefficient, α, and extinction coefficient, k, of a CdSe thin film of t = 4950Å and grown at $T_s = 523K$ at selected wavelengths.

λ (nm)	n_1	m	m_0	n	α (cm^{-1}) in 10^4	k
741(max)	3.22	4.3	4	2.99	1.79	0.106
781(min)	3.12	3.95	3.5	2.76	1.39	0.086
850(max)	3.01	3.5	3	2.57	1.16	0.078

Table 5.4: Optical band gap (E_g) values of CdSe thin films deposited at different T_s and of different thickness (t).

Thickness of the film (t)	T_s of deposition	Optical band gap (E_g) in eV
2000Å	573K	1.70
	523K	1.71
	473K	1.71
	423K	1.72
2300Å	473K	1.69
2100Å		1.70
1950Å		1.70
1750Å		1.72

$$\alpha h\nu = A_a(h\nu - E_g)^{1/2} \qquad (5.30a)$$

or to forbidden direct transitions described by

$$\alpha h\nu = A_f(h\nu - E_g)^2 \qquad (5.30b)$$

where hν is the incident photon energy, E_g represents the energy band gap and A_a & A_f are characteristic parameters, independent of photon energy, for respective transitions.

Fig 5.15(a) shows $(\alpha h\nu)^2$ vs hν plots of CdSe films having constant thickness and grown at different T_s. Fig 5.15(b) shows similar plots of CdSe thin films having different thickness and grown at constant elevated T_s. The values of α are found to be strongly dependent on hν. The graphs of $(\alpha h\nu)^{1/2}$ vs hν instead of $(\alpha h\nu)^2$ vs hν are found not to lead to straight lines, which supports the direct nature of fundamental band-to-band transitions. It means that vacuum deposited CdSe thin films have a direct band gap, which is in accordance with the energy band model of CdSe proposed by Kobayashi et al. /53/ The values of band gap are determined by extrapolating the linear portions of the respective curves to $(\alpha h\nu)^2 = 0$. The band gap values are presented in Table 5.4 and these values ranged between 1.69 and 1.72 eV, which is in close agreement with the reported values /43,54 - 56/. It is observed that there is decrease of band gap with increase of film thickness. Band gap value decreases with the

increase of T_s also which is likely due to increase of particle size and decrease in the strain values /57/.

5.4 Conclusions

Thermally deposited thin films of CdSe are found to be characterized by direct optical transitions at 1.71 eV. Excitations observed around 0.41 eV may be attributed to its native defects. The maximum photocurrent peak in spectral response of CdSe rises with T_s and t.

The growth of photocurrent in CdSe thin films indicates a very fast rise which is followed by comparatively slow increase of photocurrent to reach the state of saturation. The decay process also shows fast decrease in initial state accompanied by slow exponential decay. The rise and decay times of photocurrent are found to be dependent on intensity of illumination and applied bias voltage.

The nature of slow decay curves shows that trapping centers are responsible for controlling the photocurrent. In CdSe thin films both shallow and deep traps are found to be available. From the evaluated values of trap depth (E) it is observed that trap depths E_1 & E_2 are not single valued and there is a quasi-continuous distribution of various traps. The study also confirms that the resultant increase in photoconductivity is because of two factors one due to increase of photo generated carriers and the other due to increase of effective mobility, which is known as the barrier modulation.

The shape of the transmission spectra is influenced by the preparation conditions of the films and post deposition treatment. The spectral dependence of refractive index for CdSe thin films indicates a normal dispersion. The calculated values of energy gap range between 1.69 and 1.72eV. The band gap transitions in the films deposited on the glass substrate depend critically on the film thickness and T_s.

5.5 References

1. K. C. Sarma, R. Sarma and J. C. Garg, *Jap. J. Appl. Phys.*, 31, 1992, 742.
2. K. C. Sathyalatha, S. Uthanna and P. Jayarama Reddy, *Thin Solid Films*, 174, 1989, 233 - 238
3. P. Bhattacharya, *Semiconductor Optoelectronic Devices*, Prentice- Hall of India (P)

Ltd. 1995, New Delhi, P-130.

4. T. Nagatomo, Y. Maruta and O. Omoto, *Thin Solid Films*, 192, 1990, 17
5. I. R. Makelvey and R. L. Laugini; *Jour. Appl. Phys.*, 25(5), 1954, 634.
6. R. H. Bube; *Photoconductivity of Solids*, Wiley, N. Y., 1960, Chap. 9.
7. K. N. Shreekanthan, B. V. Rajendra, V. B. Kasturi and G. K. Shivakumar, *Cryst. Res. Technol.*; 38(1), 2003, 30.
8. A. Goswami; *Thin Film Fundamentals*, New Age International (P) Ltd., New Delhi, 1996.
9. J. Piprek; *Semiconductor Optoelectronic Devices*, Academic Press, Published by Elsevier Ind. Pvt. Ltd., New Delhi, 2005.
10. R. E. Halsted, M. R. Lorenz, B. Segall, *J. Phys. Chem. Solids*; 22, 1961, 109.
11. J. J. Hophreld, *J. Phys. Chem. Solids*, 10, 1959, 110.
12. C. Konark, J. Diminiger and V. Prosser in *II-VI Semiconductor Compounds*, Editor D. G. Thomsan, W. A. Banjamin, Inc. NY, 1967, 850
13. H. L. Kwok and W. C. Siu, *Thin Solid Films*; 61, 1979, 259.
14. K. R. Murali, P. Elango and P. Gopalakrishan, *Mat. Chem. and Phys.*, 96, 2006, 103.
15. G. K. M. Thutupalli and S. G. Tomlin, *J. Phys. D.* 9, 1976, 1639.
16. Ben. G. Streetman, *Solid State Electronic Device*, Prentice-Hall of India(P) Ltd, New Delhi 1995.
17. D. Nesheva, R. Reynolds, Z. Aneva, C. Main and Z. Levi, *J. Opto. Adv. Mat.*; 7(1), 2005, 517.
18. Y. Yodogawa, K. Shimizu and H. Kanamori, *Jpn. J. Appl. Phys.*; 12(5), 1973, 711.
19. R. H. Bube, *Photoconductivity of Solids*, John Wiley and Sons Inc. N.Y. 1960, 230
20. S. Devi and S. G. Prakash, *Ind. J. Pure and Appl. Phys.* 30, 1992, 18.
21. S. M. Ryvkin, *Photoelectric Effect in Semiconductors*, Consultant Bureau, N.Y., 1969
22. Z. Porada and E. Schabowska; *Thin Solid Films*, 66, 1980, L-55
23. A. Rose; *Concept in Photoconductivity and Allied Problem*, Interscience, N. Y., 1963.
24. P. S. Kireev, *Semiconductor Physics*, MIR Publishers, Moscow, 1978, 492
25. M. Buragohain and K. Barua, *Ind. J. Phys.* 59A, 1985, 178-184.
26. H. O. Yadav, T. S. Varadarajan, M. Mohanty, B. N. Pattanaik and L. N. Pattnaik,

Solar Energy Materials and Solar Cells, 35, 1994, 341-346.

27. P. K. Kalita, B. K. Sarma and H. L. Das; *Ind. Jour. Pure and Appl. Phys.*, 37, 1999, 885.
28. L. Kindleysides and J. Wood; *Jour. Phys. D: Appl. Phys.*, 3, 1970, 451.
29. A. Serpi; *Jour. Phys. D: Appl. Phys.*, 9, 1976, 1881
30. R. H. Bube; *Photoconductivity of Solids*, Wiley, N. Y., 1960, p 273.
31. S. M. Ryvkin; *Photoelectric Effects in Semiconductors*, Consultants Bureau, N. Y., 1969,Chap 5&6, P 88-155.
32. J. T. Randall and M. H. F. Wilkins; *Proc. Roy. Soc.* A 184, 1945, 366.
33. B. N. Srivastava and S. Singh, *Ind. J. Pure & Applied Phys.*, 8, 1970, 716.
34. R. H. Bube; *Photoconductivity of Solids*, Wiley, N. Y., 1960, p278
35. R. H. Bube; *Physics and Chemistry of II- VI Compounds*, (Eds.) M. Aven and J. Prener, North Holland, Amsterdam, 1967, p 660.
36. S. S. Devlin; *Physics and Chemistry of II- VI Compounds* (Eds.) M. Aven and J. Prener, North Holland, Amsterdam, 1967, p 589.
37. S. S. Devlin; *Physics and Chemistry of II- VI Compounds*, (Eds) M. Aven and J. Prener, North Holland, Amsterdam, 1967, p 587.
38. R. H. Bube; *Photoconductivity of Solids*, Wiley, N. Y., 1960, 61.
39. P. K. Kalita, B. K. Sarma and H. L. Das; *Bull. Mater Sci.*, 26, 2003, 613.,
40. R. Sarma, N. Mazumdar and H. L. Das, *Ind. J. Phys.*, 78A, 2004, 389
41. R. H. Bube; *Physics and Chemistry of II- VI Compounds*, (Eds.) M. Aven and J. Prener, North Holland, Amsterdam, 1967, Chap. 13.
42. A. Grabowski, M. Nowak, P. Tzanetakis, *Thin Solid Films*, 283, 1996, 77.
43. D. P. Padiyan, A. Marikani and K. R. Murali, *Mat. Chem. and Phys.*, 78, 2002, 51-58
44. K. Sen, R. S. Srivastava, D. P. Jashi and V. K. Goyal; *Phys. Status Solidi* (a) 75, 1983, 657.
45. B. P. Tyagi and K. Sen; *Phys. Status Solidi* (a) 75, 1982, 679
46. A. Goswami; *Thin Film Fundamentals*, New Age International (P) Ltd., New Delhi, 1995, Chap 11, p 410.
47. J. N. Hodgson, *Optical Absorption and Dispersion in Solids*, London Chapman and Hall, 1970.

48. Z. Ynping, Z. Chuang, Ge Xinshi and L. Xingang , *J. Phys. D: Appl. Phys*, 25, 1992, 1004

49. R. Swanpoel, *J. Phys. E: Sci. Instrum.* 16, 1983, 1214.

50. E. Marquez, J. Ramirez-Malo, P. Villares, R. Jimbnez-Garay, (P J S Ewen and A E Owen), *J. Phys. D: Applied Phys*, 25,1992, 535.

51. K. L. Chopra, *Thin Film Phenomena,* New York : McGraw-Hill, 1969.

52. J. I. Pankove, *Optical Processes in Semiconductors*, New York, Dover Pub. Inc. 1971, 34.

53. A. Kobayashi, O. F. Sankey, S. M. Volz and J. D. Dow, *Phys. Rev. B*, 28, 1983, 935

54. K. R. Murali, K. Srinivasan and D. C. Trivedi, *Mat. Sci. & Engineering B*; 111, 2004, 1-4

55. K. R. Murali, K. Srinivasan and D. C. Trivedi, *Materials Letters*, 59, 2005, 15-18.

56. C. Baban, G. I. Rusu and P. Prepelita, *J. Optoele. Adv. Mat.*, 7(2), 2005, 817-821.

57. S. Venkatachalam, D. Mangalaraj, Sa. K. Narayandass, K. Kim and J. Yi, *Physica B*, 358, 2005, 27-35.

****